



**HAL**  
open science

## Recent advances in catalytic oxidation of 5-hydroxymethylfurfural

Deyang Zhao, Ting Su, Yantao Wang, Rajender S. Varma, Christophe Len

► **To cite this version:**

Deyang Zhao, Ting Su, Yantao Wang, Rajender S. Varma, Christophe Len. Recent advances in catalytic oxidation of 5-hydroxymethylfurfural. *Molecular Catalysis*, 2020, 495, pp.111133 -. 10.1016/j.mcat.2020.111133 . hal-03491658

**HAL Id: hal-03491658**

**<https://hal.science/hal-03491658>**

Submitted on 24 Aug 2022

**HAL** is a multi-disciplinary open access archive for the deposit and dissemination of scientific research documents, whether they are published or not. The documents may come from teaching and research institutions in France or abroad, or from public or private research centers.

L'archive ouverte pluridisciplinaire **HAL**, est destinée au dépôt et à la diffusion de documents scientifiques de niveau recherche, publiés ou non, émanant des établissements d'enseignement et de recherche français ou étrangers, des laboratoires publics ou privés.



Distributed under a Creative Commons Attribution - NonCommercial 4.0 International License

## Recent advances in catalytic oxidation of 5-hydroxymethylfurfural

Deyang Zhao<sup>a,b</sup>, Ting Su<sup>b,c</sup>, Yantao Wang<sup>d</sup>, Rajender S. Varma<sup>e</sup> and Christophe Len<sup>b,f,\*</sup>

[a] School of Chemistry and Materials Science, Ludong University, Yantai 264025, China

[b] Chimie ParisTech, PSL Research University, CNRS, Institute of chemistry for Life and Health Sciences, 11 rue Pierre et Marie Curie, F-75005 Paris, France

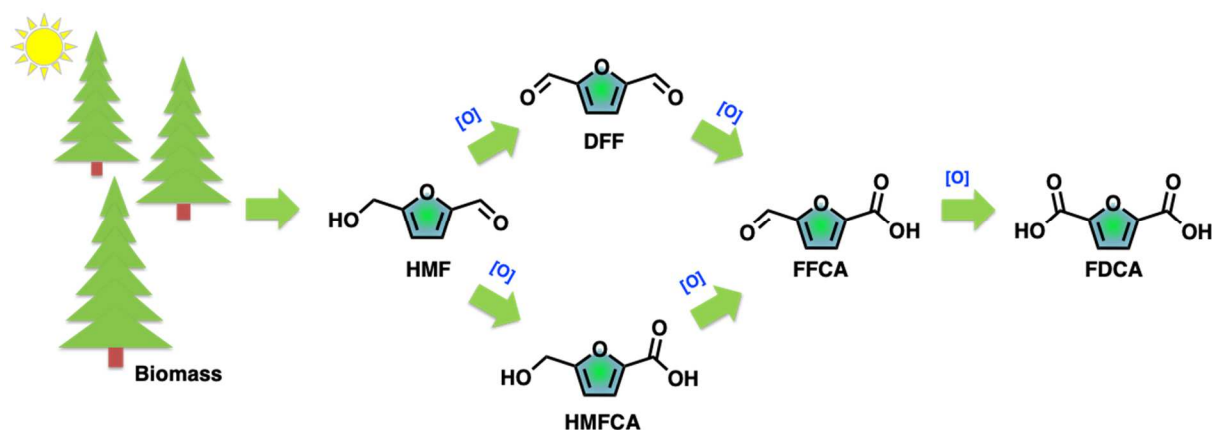
[c] Green Chemistry Centre, College of Chemistry and Chemical Engineering, Yantai University, Yantai 264005 China

[d] School of Resources Environmental & Chemical Engineering, Nanchang University, Nanchang 330031, China

[e] Regional Center of Advanced Technologies and Materials, Palacky University, Šlechtitelů 27, 783 71, Olomouc, Czech Republic

[f] Université de Technologie de Compiègne, F-60200 Compiègne, France

*E-mail* address: [christophe.len@chimieparistech.psl.eu](mailto:christophe.len@chimieparistech.psl.eu) (C. Len)



**Abstract:** 5-Hydroxymethylfurfural (HMF) has been considered as one of the most promising versatile biomass based platform molecules. This review discusses recent advances in catalytic oxidation of HMF towards 2, 5-furandicarboxylic acid (FDCA) as well as other

HMF oxidation intermediates: 2,5-diformylfuran (DFF), 5-hydroxymethyl-2-furancarboxylic acid (HMFCFA), 5-formyl-2-furancarboxylic acid (FFCA) deploying noble, non-noble, metal-free and biocatalytic systems in conventional batch protocols; reaction mechanisms and the reaction conditions are well deliberated. Selective HMF downstream oxidation products are obtained *via* catalyst modifications such as the nature of metal, preparative method as well the property of deployed support. HMF oxidation, an important and integral biomass-based valorization process towards valuable chemicals, deserves more attention.

**Keywords:** 5-Hydroxymethylfurfural, Catalytic oxidation, Heterogeneous catalyst, Conventional batch process

## 1. Introduction

With the rapid development of modern society, the depletion of non-renewable resources, the ensuing greenhouse effect and environmental pollution has garnered more attention, as worldwide environmental issues have started to impact the quality of human life; search for newer and greener strategies and alternative resources for the sustainable development has intensified. Lignocellulosic biomass resources are the most abundant renewable carbon resources on the planet, comprising cellulose (40-50%), hemicellulose (20-30%), lignin (10-25%) and other negligible groups (**Fig. 1**) [1]. Among them, cellulose with  $\beta$ -1,4 bonds of anhydrous glucose unit [2], through hydrolysis to glucose, *in situ* isomerization to fructose, followed by dehydration is converted to an important bio-based platform compound: 5-hydroxymethylfurfural (HMF) [3-6]. Different reviews reported general conversion of biomass such as HMF into bio-based compounds and fuels [7-9] and one is specific on the catalytic oxidation of carbohydrates [10]. Nevertheless, specific advances in catalytic oxidation of HMF were not reviewed in details.

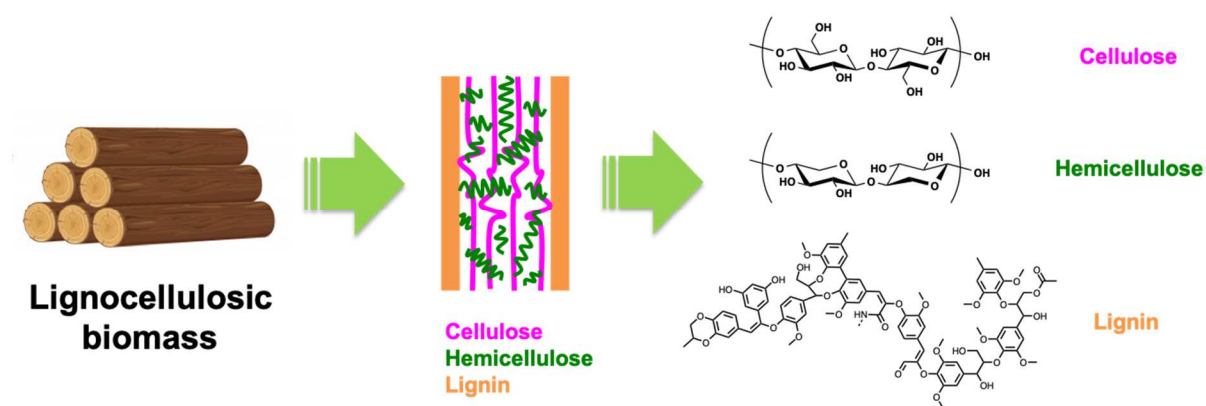
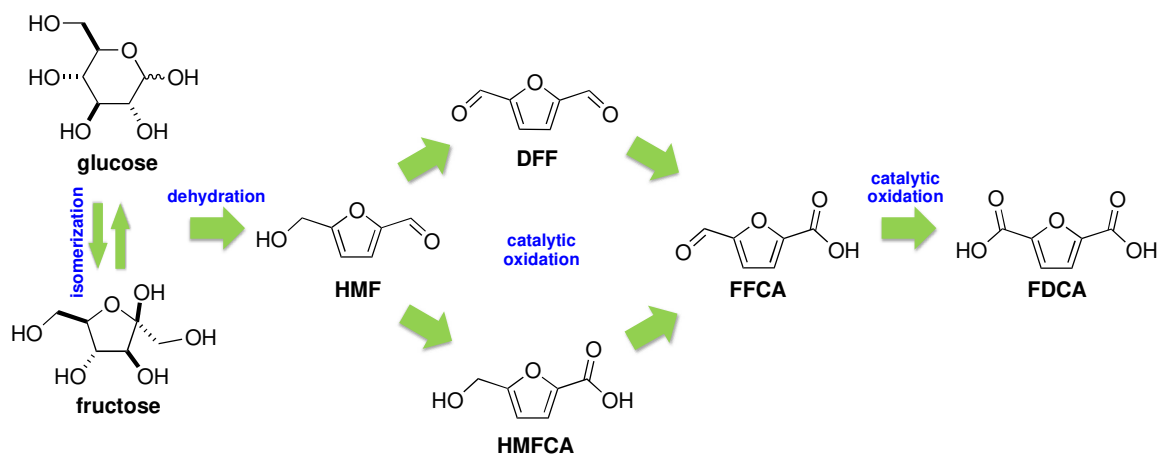


**Fig. 1.** Lignocellulosic structural units.

The oxidation of lignocellulosic platform molecules to value-added chemicals has been laid out as an efficient pathway for valorization of biomass-based compounds. Four key platform molecules namely glucose, HMF, furfural and levulinic acid, are recognized as downstream high value compounds [11,12]. Among them, 2,5-diformylfuran (DFF), 5-hydroxymethyl-2-furancarboxylic acid (HMFCFA), and 5-formyl-2-furancarboxylic acid (FFCA) are the main intermediates of HMF oxidation (**Scheme 1**); each of them is important biomass-based furan compounds with wide-spread applications. For instance, DFF is used for synthesis of ligands, pesticide, antifungal agents, fluorescent materials and new polymeric materials [13,14]. HMFCFA has been reported as an interleukin inhibitor [15], which also showed antitumoral activities [16]. Furthermore, FFCA has some unique structural advantages for the synthesis of drug derivative as attested in two patents; structures of FFCA-based drug derivatives are depicted in **Fig. 2**.



**Scheme 1.** Oxidation pathway for HMF.

The final oxidation product, 2,5-furandicarboxylic acid (FDCA), has been considered as the most promising candidate in furan family featuring the unique cyclic furan ring with appended diacid group [17]; DuPont and DSM have commented on FDCA as "a sleeping giant with unlimited potential." In 2004, US Department of Energy identified twelve bio-based platform compounds currently considered most likely to replace more than 300 petroleum-based substitution products. Due to aromatic ring's plane and rigid structure, FDCA was the only bio-based platform compound-recommended [18].

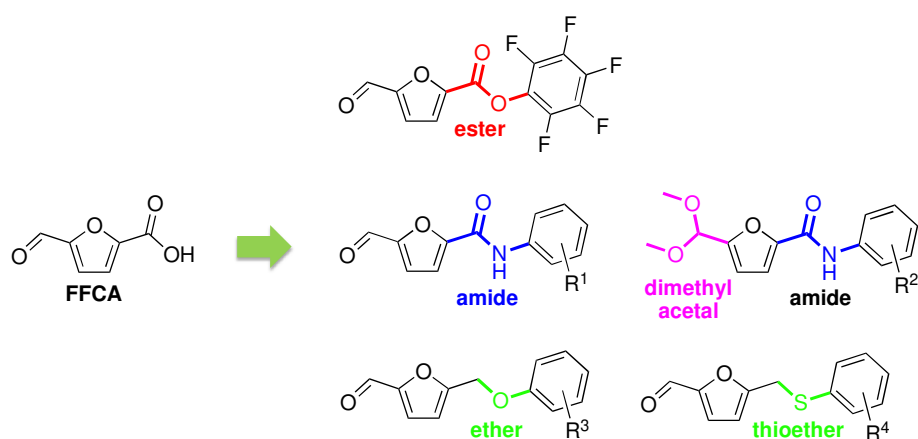
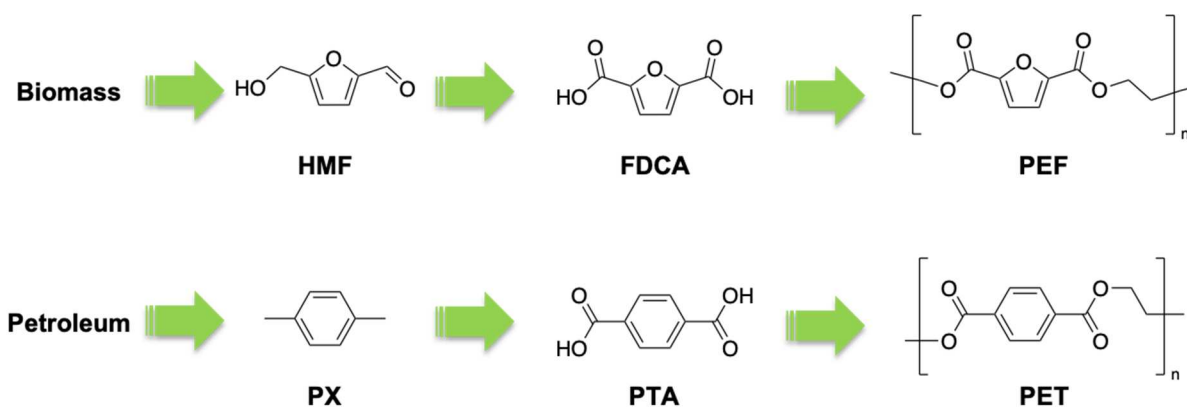


**Fig. 2.** FFCA-based drug derivatives.

2,5-Furandicarboxylic acid (FDCA)–has received significant attention due to its wider applications in many fields. For instance, in the synthesis of biochemical compounds such as succinic acid [19], 2,5-dihydroxymethylfuran, 2,5-dihydroxymethyltetrahydrofuran, 2,5-bis(aminomethyl)-tetrahydrofuran [18]. FDCA diethyl ester showed strong anaesthetic action similar to cocaine [20], FDCA dicalcium salt was reported to inhibit the growth of *Baccillus megatorium* spora [21] and FDCA-derived anilides 73 demonstrated anti-bacterial action [22]. FDCA by itself is a strong complexing agent, chelating ions such as  $\text{Ca}^{2+}$ ,  $\text{Cu}^{2+}$  and  $\text{Pb}^{2+}$  reportedly capable of-removing kidney stones [23]. In addition, FDCA has been deployed in plasticizers, coatings, adhesives, metal-organic framework materials, among others.

Remarkably, another impressive application of FDCA lies in the bio-based polymer industry as its structural similarity to p-xylene (PX) enables polymerization with diol, diamine or other monomers to produce bio-based polymer materials. For instance, polyethylene 2,5-furandicarboxylate (PEF) is an excellent biopolymer alternative to polyethylene terephthalate (PET) which is obtained from fossil-based monomer terephthalic acid (TPA) [24] (**Scheme 2**). The starting material for PEF as sourced from biomass reduces the reliance on fossil resources. Furthermore, taking into account the improved salient features such as excellent gas barrier, recyclability and extend mechanical properties than PET [25], PEF is widely employed in food and beverage packaging, and in textile fibers. The Coca Cola company has collaborated with Avantium, Danone, and ALPLA to develop and commercialize PEF bottles. In view of its extensive applications, the price of the high purity FDCA on Sigma-Aldrich is rather expensive at 102 euros (5 g), thus suggestive of extensively studies on catalytic synthesis of FDCA.



**Scheme 2.** The comparative origins of PEF and PET.

5-Hydroxymethylfurfural (HMF) as a promising starting material for FDCA production *via* chemical catalytic method started in the 19<sup>th</sup> century. A wide variety of reaction systems have been investigated for the oxidation of HMF ranging from noble metal, non-noble metal, metal-free and biocatalysts, benign oxidants like oxygen, air, H<sub>2</sub>O<sub>2</sub>, and KMnO<sub>4</sub> as well as homogeneous- and heterogeneous-based approaches under conventional batch conditions. Based on these premises, the aim of this review is centered on the most recent findings with a critical discussion on HMF oxidation to FDCA as well as other HMF oxidation intermediates. The underlying mechanisms in different catalytic systems ranging from noble-metal, non-noble metal, metal-free as well as biocatalysts under divers-reaction conditions (HMF/metal molar ratio, oxidant source and pressure, base type and amount, reaction temperature and time) are also discussed.

## 2. Oxidation of HMF to FDCA – Conventional batch processes

### 2.1. Noble metal

The oxidation of HMF to FDCA over heterogeneous catalysts in conventional batch processes has been extensively investigated and mostly, gold (Au), platinum (Pt), palladium (Pd) ruthenium (Ru) and silver (Ag) occupied were deployed.

### 2.1.1. Gold (Au)

Au as a traditional noble metal as well supported on a variety of support have been found to be very active for oxidation of HMF to FDCA [26,27]; studies have identified the best supports and reaction conditions for improving FDCA yield [28,29]. Au/CeO<sub>2</sub> showed significantly high HMF oxidation activity [30], as a series of Au- based catalysts on CeO<sub>2</sub> was studied by Albonetti et al. [31] and yield of FDCA attained was 52% under optimum condition (10 bar O<sub>2</sub>, 4eq. NaOH, 70 °C and 4 h) (**Table 1**, entry 1). With the increase in temperature from 70 to 130 °C, FDCA yield increased from 52% to 96% despite HMF/Au amount from 100 to 640 and 10 bar air (**Table 1**, entry 2). Not only the particle size of Au but also the support plays a key role in HMF oxidation in the aqueous phase; CeO<sub>2</sub> served as a superior support for HMF oxidation in numerous reports [32-36]. The easy Ce<sup>4+</sup> /Ce<sup>3+</sup> redox transition increased significant oxygen mobility and storage capacity. Additionally, higher number of oxygen vacancies on CeO<sub>2</sub> increased the proportion of cationic Au and more interfacial Lewis acidic sites. A synergistic effect between the interfacial Lewis acid, homogeneous base and neighbored Au particles promoted the oxidation reaction by efficiently activating the hydroxyl, aldehyde and molecular O<sub>2</sub> [37-40]. Au-CeO<sub>2</sub> stability experiment was performed under the optimal conditions (**Table 1**, entry 2), where HMF suffered a serious degradation during the reaction, only 20% HMFCA was obtained after the first hour; active sites may be partially blocked by organic molecules adsorbed onto the catalyst surface.

To decrease the formation of humins and enhance the catalyst's stability, HMF with 1,3-propanediol generated an HMF acetal derivative (PD-HMF) as reported by M. Kim research group [42], wherein the six-membered acetal ring can suppress the thermal decomposition and self-polymerization of HMF; PD-HMF conversion was 99% and FDCA

yield of 91% was attained after prolonged reaction time of 15 h under optimal condition (PD-HMF/Au molar ratio, 53, 5 bar O<sub>2</sub>, 2eq. Na<sub>2</sub>CO<sub>3</sub>) even at elevated temperature of 140 °C (**Table 1**, entry 3). The catalytic activity of Au/CeO<sub>2</sub> could be dramatically improved by incorporating Bi<sup>3+</sup> into the CeO<sub>2</sub> support nanostructure, due to the availability of lone pair electrons (Bi<sup>3+</sup>) which increased the Bi–O–Ce linkages together with large proportions of Ce<sup>3+</sup> centers and oxygen vacancies; nearly quantitative HMF conversion and 99% yield of FDCA (**Table 1**, entry 4) was obtained in only 2 hours over Au/Ce<sub>0.9</sub>Bi<sub>0.1</sub>O<sub>2-δ</sub> catalyst at a lower temperature (65 °C) while using a lower oxidant source pressure (1 bar O<sub>2</sub>) when compared to earlier cases (**Table 1**, entry 1 to 3).

**Table 1**

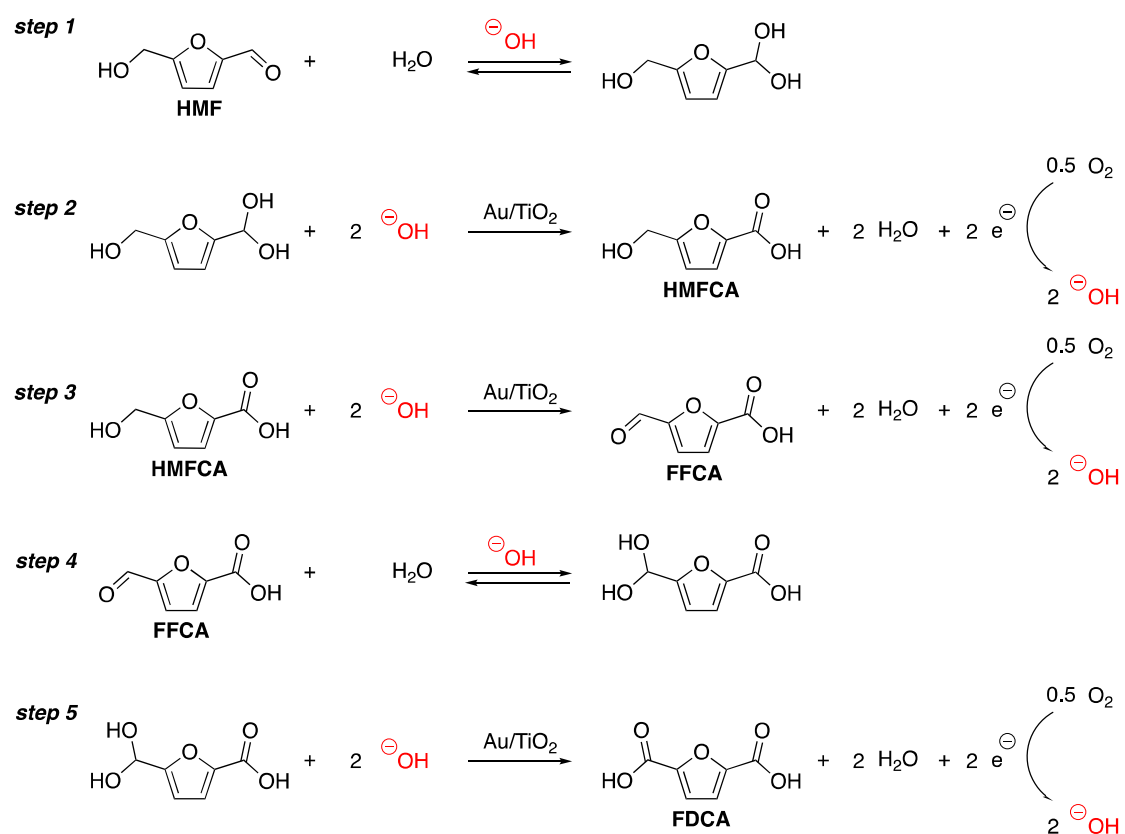
Oxidation of HMF to FDCA over Au-based catalysts.

Entry	Catalyst	HMF/metal molar ratio	Oxidant	Base [eq.]	T [°C]	Time [h]	Conv (HMF) [%]	Yield (FDCA) [%]	Ref.
1	Au/CeO <sub>2</sub>	100	O <sub>2</sub> (10 bar)	NaOH (4 eq)	70	4	100	52	[31]
2	Au/CeO <sub>2</sub>	640	air (10 bar)	NaOH (4 eq)	130	5	100	96	[41]
3	Au/CeO <sub>2</sub>	53	O <sub>2</sub> (5 bar)	Na <sub>2</sub> CO <sub>3</sub> (2 eq)	140	15	99	91	[42]
4	Au/Ce <sub>0.9</sub> Bi <sub>0.1</sub> O <sub>2-δ</sub>	149	O <sub>2</sub> (1 bar)	NaOH (5 eq)	65	2	100	99	[43]
5	Au/TiO <sub>2</sub>	110	O <sub>2</sub> (3 bar)	NaOH (5 eq)	60	6	99	85	[29]
6	Au/TiO <sub>2</sub>	150	air (10 bar)	NaOH (4 eq)	130	8	100	99	[41]
7	Au/TiO <sub>2</sub>	100	O <sub>2</sub> (10 bar)	NaOH (20 eq)	30	18	100	71	[26]
8	Au/TiO <sub>2</sub>	100	<sup>18</sup> O <sub>2</sub> (3.4 bar)	NaOH (20 eq)	25	22	100	69	[27]
9	Au-Cu/TiO <sub>2</sub>	100	air (10 bar)	NaOH (4 eq)	95	4	100	99	[44]
10	Au-Pd/IRA-743	100	air (10 bar)	Na <sub>2</sub> CO <sub>3</sub> (1 eq)	100	4	100	93	[45]

11	Au-Pd/PECN	100	O <sub>2</sub> (1 bar)	K <sub>2</sub> CO <sub>3</sub> (4 eq)	90	12	100	99	[46]
12	Au-Pd/ZOC	100	O <sub>2</sub> (3 bar)	NaHCO <sub>3</sub> (4 eq)	80	4	99	99	[47]
13	Au-Pd/Ac	200	O <sub>2</sub> (3 bar)	NaOH (2 eq)	60	2	100	95	[48]
14	Au-Pt/Ac	200	O <sub>2</sub> (3 bar)	NaOH (2 eq)	60	2	100	62	[48]
15	Au/Ac	200	O <sub>2</sub> (3 bar)	NaOH (2 eq)	60	2	100	36	[48]
16	Au-Pd/nNiO	100	O <sub>2</sub> (10 bar)	Base free	90	14	100	99	[49]
17	Au-Pd/La-CaMgAl-LDH	68	O <sub>2</sub> (5 bar)	Base free	100	4	100	99	[50]
18	Au-Pd/CNT	100	O <sub>2</sub> (5 bar)	Base free	100	18	100	91	[51]
19	Au/MgO	50	O <sub>2</sub> (16 bar)	Base free	110	2	99	91	[52]
20	Au/HT	40	O <sub>2</sub> (50 mL min <sup>-1</sup> )	Base free	93	7	99	99	[53]
21	Au/HT-Ac	100	O <sub>2</sub> (5 bar)	Base free	100	24	100	99	[54]
22	Au/ZrO <sub>2</sub>	384	air (50 bar)	NaOH (4 eq)	125	5	100	89	[55]
23	Au/SiO <sub>2</sub>	72	O <sub>2</sub> (10 bar)	NaHCO <sub>3</sub> (2 eq)	90	5	99	74	[56]
24	Au/Al <sub>2</sub> O <sub>3</sub>	100	O <sub>2</sub> (3 bar)	NaOH (4 eq)	70	4	100	99	[57]

---

TiO<sub>2</sub> is another common support that has captured attentions for HMF oxidation to FDCA [58-60]. Cai et al. [29] reported Au supported on TiO<sub>2</sub>, CeO<sub>2</sub>, Mg(OH)<sub>2</sub> and HY zeolite to produce FDCA in water under mild conditions (60 °C, 3 bar O<sub>2</sub>), 85% FDCA could be observed (**Table 1**, entry 5). Higher yield of FDCA was attained (99% yields) (**Table 1**, entry 6) when temperature and oxidant were both increased (60 °C to 130°C, 3 bar O<sub>2</sub> to 10 bar air) despite the increase of HMF/Au molar ratio from 110 to 150. TiO<sub>2</sub> displayed much higher HMF oxidation performance when compared to other supports, such as Fe<sub>2</sub>O<sub>3</sub> or activated coal which afforded FDCA 15% and 44%, respectively under the same reaction conditions [41]. Gorbanev et al. [26] also reported the formation of FDCA and the yield of intermediate HMFCFA depend on the amount of added base and the oxygen pressure; 71% FDCA yield was attainable under room temperature with addition of more base (20 eq.) (**Table 1**, entry 7). Davis et al. [27] achieved 69% FDCA yield (**Table 1**, entry 8) under almost the same optimal condition (**Table 1**, entry 7) with the delineation of mechanism using the labeling experiments conducted with <sup>18</sup>O<sub>2</sub> and H<sub>2</sub><sup>18</sup>O. As seen from Scheme 4, hydroxyls ions play an important role in HMF oxidation which can catalyze aldehyde groups originating from HMF and FFCA to geminal diols in water (**Scheme 3**, steps 1 and 4). For the next step, the H atom from C-H and O-H groups of alcohol or geminal diol can be abstracted by OH<sup>-</sup> ions, which are adsorbed on Au surface or at the Au based support interface, to afford carbonyl and carboxylic groups, respectively (**Scheme 3**, steps 2, 3 and 5). Then, the hydroxyl groups could be regenerated by oxygen scavenged electrons (**Scheme 3**, steps 2, 3 and 5, right side).



**Scheme 3.** Overall mechanism for oxidation of HMF-to FDCA.

Since Au supported on CeO<sub>2</sub> and TiO<sub>2</sub> were reported to lose activity rapidly due to the active sites being blocked by organic adsorption, so called humins [41], and Au leaching [26], the bimetallic Au-Cu catalysts displayed a superior activity and stability as compared to monometallic Au, as was shown by Pasini et al. [44]. The obtained yield of FDCA was 99% at 95 °C, in 4 h (**Table 1**, entry 9). Notably, after reaction, the performance of Au-Cu catalysts showed no significant loss of activity and selectivity. Bimetallic Au-Pd alloy nanoparticles supported on basic anion-exchange resin (AER) also performed well [45,46] as HMF was oxidized to FDCA in 93% yield (**Table 1** entry 10) under optimum conditions with 1:1 ratio of Au-Pd alloy nanoparticles over Amberlite IRA-743 resin. In a comparative study, bimetallic performance with simple mixture of the two monometallic catalysts (1% Au/IRA-743 plus 1% Pd/IRA-743) gave only a 52% FDCA selectivity under the identical conditions. The bimetallic catalyst could be used 6 times without any significant loss of activity. Wang et

al. [46] reported MPIL-based ionic copolymers (amphiphilic PECN) supported Au-Pd alloy NPs as catalyst which could increase the catalytic performance, under mild condition, 100% HMF conversion and 99% FDCA achieved (**Table 1**, entry 11). The encouraging performance has been attributed to the hydrophilic and hydrophobic properties on the support surface. Zinc hydroxycarbonate (ZOC) was found to be another good support for improving the yield of FDCA [47], the basicity property of ZOC support being an important factor on the enhancement of catalytic activity. Au-Pd/ZOC with an Au:Pd (molar ratio 1:1) showed the highest catalytic activity towards HMF oxidation in water at relative mild conditions, attaining > 99% yield of FDCA (**Table 1**, entry 12). Noticeable, recyclability of Au-Pd/ZOC revealed no significant loss in seven consecutive runs. Villa et al. [48] demonstrated the modification of Au/Ac catalyst by adding Pt or Pd for HMF oxidation to FDCA (**Table 1**, entries 13-15); bimetallic catalysts Au-Pd/Ac showed an enhanced activity when compared to the monometallic Au/Ac and bimetallic Au-Pt/Ac (the yield of FDCA 95% vs. 36% and 62%, respectively). In terms of catalyst's durability metric, Au/Ac was not stable in recycling experiments. However, the stability and activity could be dramatically enhanced by alloying Au with Pd, Au<sub>8</sub>Pd<sub>2</sub>/Ac can be recycled for up to while 5 times maintaining 99% selectivity to FDCA. These experiments proved sufficiently that the Au alloy-based catalyst can not only enhance the HMF oxidation performance but also the catalyst durability.

From the perspective of green chemistry, the aerobic oxidation of HMF to FDCA under base-free condition is highly desirable. An efficient and stable basic nanosized NiO supported Au-Pd nanoparticles (6:4 Au/Pd atomic ratio) were reported for HMF oxidation with 100% HMF conversion and 99% FDCA (**Table 1**, entry 16) under optimized condition in homogeneous base-free system [49]. The impressive results were attributed to the significant synergistic effects between Au and Pd in the alloy as well as NiO. La-doped Ca-Mg-Al layered double hydroxide (La-CaMgAl-LDH) supported AuPd bimetallic nanoparticles [50]

under base-free conditions was investigated for the aerobic HMF to FDCA, 99% FDCA yield obtained under optimized reaction conditions (**Table 1**, entry 17). The encouraging performance of the catalyst is believed to be correlated with not only the higher surface basicity of La-CaMgAl-LDH support but also the synergy between Au-Pd atoms. Several other basic support as matrix were examined to support Au-Pd like Au-Pd/Al<sub>2</sub>O<sub>3</sub>, Au-Pd/MgO, Au-Pd/HT and Au-Pd/CNT by Wan et al. [51]; Au-Pd/CNT showed the highest efficiency as a recyclable catalyst for HMF conversion to FDCA under base-free conditions as quantitative HMF conversion with 91% FDCA yield was discerned over the Au-Pd/CNT after 18 h (**Table 1**, entry 18). The functionalization of CNT surface was crucial for the formation of FDCA, the carbonyl/quinone and/or phenol groups enhanced the adsorption of HMF and the possible intermediates onto the CNT surfaces, thus increasing the catalytic performance. In contrast, the carboxyl groups on the surface are disadvantageous for the adsorption of these molecules.

In this regard, Donoeva et al. [61] compared FDCA selectivity using Au supported on both acidic and basic carbon materials. The results showed basic carbon supports that were positively charged under reaction conditions displayed a higher adsorption of substrate, the local concentration of hydroxyl ions which acted as co-catalysts attributed to the synergy with Au, thus enhancing the catalyst's performance. Negatively charged surface groups of acidic carbons repel hydroxyls and the intermediate, which leads to lower catalytic performance and a low selectivity towards FDCA.

Monometallic Au NPs catalyst under base-free condition have also been widely reported. Au NPs supported on MgO, NiO, TiO<sub>2</sub>, ZrO<sub>2</sub>, CeO<sub>2</sub> were prepared for the oxidation of HMF [52] where Au/MgO was identified as the most efficient-in catalyst screening with quantitative HMF conversion and 91% FDCA yield (**Table 1**, entry 19); FDCA yield (in the bracket) followed the order MgO (91%) > NiO (33%) > TiO<sub>2</sub> (11%) ≈ ZrO<sub>2</sub> (6%) ≈ CeO<sub>2</sub>

(8%). It was revealed that the support played a crucial role in the oxidation reactions and the activity related to the basic sites on the surface of a metal oxide. Alkali-free Mg-Al hydrotalcites were identified as excellent solid base catalysts for the aerobic oxidation of HMF to FDCA and garnered much attention in recent years [53,54, 62-64]. Noticeably, Gupta et al. [53] reported that Au/HT was a highly effective heterogeneous catalyst for selective oxidation of HMF to FDCA; complete HMF conversion and the highest FDCA yield was obtained using 50 mL/min oxygen flow as oxidant (**Table 1**, entry 20) and the catalyst could be reused at least three times without significant loss of activity and selectivity.

In this context, physical milling of HT and AC as matrix support for Au also showed good catalytic performance with 99% FDCA yield in 24 h under base-free conditions (**Table 1**, entry 21) [54], catalyst was stable up to 6 cycles without any decrease in selectivity for FDCA. The impressive performance was attributed to a large surface area, basic sites, surface hydroxyl and carbonyl groups on the surface of HT-AC, being very ideal for high dispersion of Au nanoparticles and adsorption of HMF as well as intermediates.

Other support such as ZrO<sub>2</sub>, Al<sub>2</sub>O<sub>3</sub>, SiO<sub>2</sub> with homogeneous base were rarely reported (**Table 1**, entries 22-24). Au/ZrO<sub>2</sub> afforded 89% yield of FDCA under optimum condition (**Table 1**, entry 22). Gupta [53] reported that Au/SiO<sub>2</sub> in the absence of a base was inactive for the oxidation of HMF. Later, Masoud [56] prepared Au/SiO<sub>2</sub> produced 74% FDCA yield under base conditions (**Table 1**, entry 23). Noticeably, Megias-Sayago et al. [57] prepared Au/Al<sub>2</sub>O<sub>3</sub> through direct anionic exchange (DAE) method, which enabled the fast and direct interaction between Au species and the support leading to a very efficient and active catalyst for HMF oxidation; 99% FDCA yield was achieved (**Table 1**, entry 24). The stability and reusability study of the catalyst in 5 subsequent cycles without any noticeable deactivation, showed its prowess as an efficient and novel catalyst for this synthesis methodology.

### 2.1.2. Palladium (Pd)

Au-Pd bimetallic catalyst demonstrated efficient catalytic activation towards HMF oxidation and stability than monometallic Pd based catalyst as listed in Table 1 [65-66]. Nevertheless, monometallic Pd based catalysts were still—widely investigated for HMF oxidation initially. Starting with variety of carbon-based supports, Davis et al. [67] compared Pd/C and Au/C for HMF oxidation under the identical reaction condition (7 bar O<sub>2</sub>, 2 eq. NaOH, 70 °C, 4 h), Pd/C yielded FDCA 71% (**Table 2**, entry 1). The yield of the intermediate product HMFCFA—was 92% while the yield of FDCA was only 8% when using Au/C. It revealed the oxidation of HMF aldehyde side chain to carboxylic group was more efficient over Au/C. Pd oxidized and activated the alcohol side chain of HMFCFA to FDCA effectively. Another carbon-based support (through carbonization of glucose) as matrix, Pd/CC—reportedly displayed efficient catalytic activation towards HMF oxidation to FDCA, 85% FDCA achieved (**Table 2**, entry 2) [68].-Espinosa et al. [69] investigated Pd supported on few-layers graphene (FLG), carbon nanotubes (CNT) and carbon nanofibers (CNF) to determine how the carbon-based support with different structures influence the catalytic activity on HMF oxidation to FDCA. Pd supported on FLG was initially the most active catalyst for HMF oxidation (**Table 2**, entries 3-5) in 5 hours, but it undergoes deactivation to significant extent in catalyst recycling experiment. However, Pd/CNF presented a compromised balance performance between catalytic activity and stability up on reuse results. It was revealed that Pd dispersion was not the only parameter, the nature and proportion of the basal, non-basal and defective planes of the support were of additional decisive importance in determining the activity and stability of the Pd-based carbon support. Other C-based catalyst comprising Pd, Bi, and Te supported on activated carbon were shown to be highly effective for the oxidation of diverse benzylic and aliphatic primary alcohols [70], HMF oxidation under optimum conditions, afforded 95% yield of FDCA (**Table 2**, entry 6); extended stability under

continuous flow conditions for oxidation bodes well for the application on large-scale. Pd supported on nitrogen and phosphorus codoped graphene sheets (HPGSs)-Pd/HPGSs has been reported [71]. The graphene sheets were produced by thermal pyrolysis under an inert atmosphere at 1000 °C, followed by decomposition and condensation to C<sub>3</sub>N<sub>4</sub>-like intermediate and subsequent release of nitrogen, oxygen, and phosphorus atoms to generate a large space and mesopores to establish a porous structure. It was demonstrated that HPGSs enhanced the fraction of surface Pd<sup>2+</sup> species, thus increased catalytic performance as fully HMF conversion and 83% FDCA yield could be achieved (**Table 2**, entry 7).

Pd/PVP catalyst with a Pd diameter of 1.8 nm produced highest 90% FDCA yield after 6 h at 100 °C (**Table 2**, entry 8), while FDCA yield diminished to 81% for Pd NPs diameter with a size of 2.0 nm and finally to 61% for the 6.3 nm sized Pd NPs [72]; smaller size of Pd NPs dispersion was more efficient for the HMF oxidation reaction. Another study deploying PVP-stabilized single-crystalline Pd examined the facet- and size-dependent effect on the catalytic performance [73]. The facet effect of Pd nanocrystals was found to be another pivotal factor, Pd-NCs enclosed by {111} facets were more efficient than Pd-NCs enclosed by {100} facets towards HMF aerobic oxidation. Furthermore, Pd/ PVP deposited on four different kind of metal oxides (TiO<sub>2</sub>,  $\gamma$ -Al<sub>2</sub>O<sub>3</sub> KF-Al<sub>2</sub>O<sub>3</sub> and ZrO<sub>2</sub>-La<sub>2</sub>O<sub>3</sub>) were also examined [74]; Pd NP deposited on Al<sub>2</sub>O<sub>3</sub> or TiO<sub>2</sub> (**Table 2**, entries 9-10) led to lower FDCA yields of 78% and 52%, respectively while Pd/KF-Al<sub>2</sub>O<sub>3</sub> could afford 91% FDCA yield (**Table 2**, entry 11). Unfortunately, in view of the catalyst stability, FDCA yield decreased from 91% to 55% during the first and the second run but for Pd/ZrO<sub>2</sub>-La<sub>2</sub>O<sub>3</sub> material (**Table 2**, entry 12), the FDCA yield decreased slightly from 90% to 86% after three runs, exhibiting good catalytic performance and stability.

**Table 2**

HMF oxidation to FDCA over Pd based catalyst.

Entry	Catalyst	HMF/metal molar ratio	Oxidant	Base [eq.]	T [°C]	Time [h]	Conv (HMF) [%]	Yield (FDCA) [%]	Ref.
1	Pd/C	150	O <sub>2</sub> (7 bar)	NaOH (2 eq)	70	4	100	71	[67]
2	Pd/CC	16	O <sub>2</sub> (20 mL min <sup>-1</sup> )	K <sub>2</sub> CO <sub>3</sub> (3 eq)	140	30	100	85	[68]
3	Pd/FLG	83	O <sub>2</sub> (5 bar)	K <sub>2</sub> CO <sub>3</sub> (2 eq)	160	5	100	85	[69]
4	Pd/CNT	83	O <sub>2</sub> (5 bar)	K <sub>2</sub> CO <sub>3</sub> (2 eq)	160	5	100	60	[69]
5	Pd/CNF	83	O <sub>2</sub> (5 bar)	K <sub>2</sub> CO <sub>3</sub> (2 eq)	160	5	100	70	[69]
6	Pd-Bi-Te/C	100	O <sub>2</sub> (1 bar)	KOH (3.4 eq)	50	6	100	95	[70]
7	Pd/HPGSs	60	O <sub>2</sub> (500 mL min <sup>-1</sup> )	NaOH (1 eq)	50	6	100	83	[71]
8	Pd/PVP	100	O <sub>2</sub> (1 bar)	NaOH (1.2 eq)	90	6	100	90	[72]
9	Pd/TiO <sub>2</sub>	100	O <sub>2</sub> (1 bar)	NaOH (1.2 eq)	90	8	100	52	[74]
10	Pd/Al <sub>2</sub> O <sub>3</sub>	100	O <sub>2</sub> (1 bar)	NaOH (1.2 eq)	90	8	100	78	[74]
11	Pd/KF-Al <sub>2</sub> O <sub>3</sub>	100	O <sub>2</sub> (1 bar)	NaOH (1.2 eq)	90	8	100	91	[74]

12	Pd/ZrO <sub>2</sub> -La <sub>2</sub> O <sub>3</sub>	100	O <sub>2</sub> (1 bar)	NaOH (1.2 eq)	90	8	100	90	[74]
13	Pd/C-Fe <sub>2</sub> O <sub>3</sub>	56	O <sub>2</sub> (1 bar)	K <sub>2</sub> CO <sub>3</sub> (0.5 eq)	80	4	98	91	[75]
14	Pd/C@Fe <sub>3</sub> O <sub>4</sub>	27	O <sub>2</sub> (20 mL min <sup>-1</sup> )	K <sub>2</sub> CO <sub>3</sub> (0.5 eq)	80	6	99	87	[76]
15	γ-Fe <sub>2</sub> O <sub>3</sub> @HAP-Pd(0)	43	O <sub>2</sub> (30 mL min <sup>-1</sup> )	K <sub>2</sub> CO <sub>3</sub> (0.5 eq)	100	6	97	93	[77]
16	Pd/HT	21	O <sub>2</sub> (100 mL min <sup>-1</sup> )	Base free	100	8	100	100	[78]
17	Pd-Pt-PVP/HT	75	O <sub>2</sub> (40 mL min <sup>-1</sup> )	Base free	95	11.5	100	100	[79]
18	Ni <sub>0.9</sub> Pd <sub>0.1</sub>	20	Air bubbling	Na <sub>2</sub> CO <sub>3</sub> (1 eq)	80	4	100	86	[80]

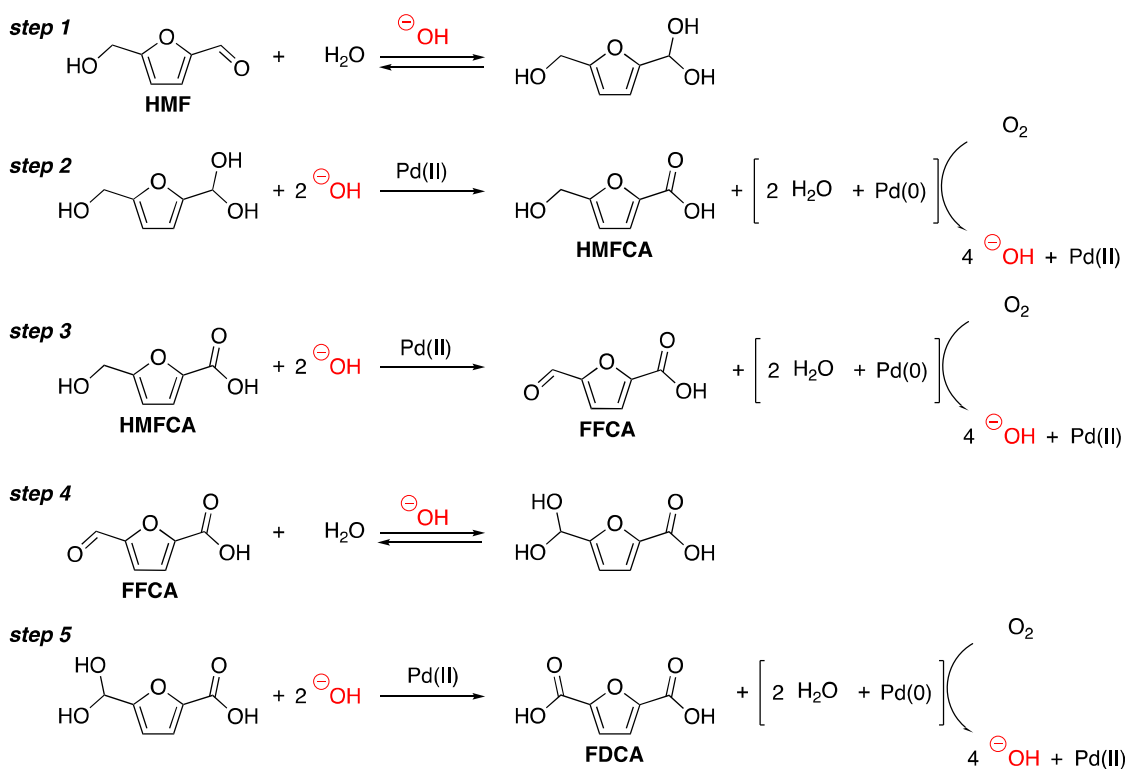
---

Zhang group [75-77] has made several contributions to the valorization of biomass-based compounds. A magnetically separable catalyst (Pd/C–Fe<sub>3</sub>O<sub>4</sub>) exhibited an impressive FDCA yield (92%) under optimized condition (**Table 2**, entry 13); catalyst was easily collected by an external magnet and reused without significant loss of catalytic activity [75]. Another similar magnetic catalyst Pd/C@Fe<sub>3</sub>O<sub>4</sub> was successfully prepared by the deposition of Pd nanoparticles on the core–shell structure of C@Fe<sub>3</sub>O<sub>4</sub> composites [76] which afforded nearly quantitative HMF conversion with 86.7% FDCA yield (**Table 2**, entry 14) and barely any loss of its activity up on recycling. Again,  $\gamma$ -Fe<sub>2</sub>O<sub>3</sub>@HAP-Pd(0) magnetic catalyst led to 93% FDCA yield (**Table 2**, entry 15), while retaining its catalytic effectiveness in five consecutive runs [77]. These efforts (**Table 2**, entries 13-15) provided a greener and sustainable option for the production of valuable chemicals from renewable resources with easy catalyst recovery and durable catalyst performance.

Base-free catalytic systems deserved attention as well. Wang et al. [78] reported a series of solid base Mg/AlCO<sub>3</sub> hydrotalcites with varying Mg/Al molar ratios and deployed them as matrixes to support Pd nanoparticles. Not only Pd loading amount, but also the Mg/Al molar ratio had significant influences on the catalytic activity and selectivity; -2% Pd/HT exhibited the highest activity and FDCA selectivity, > 99.9% FDCA yield were attained in 8 h under mild conditions (**Table 2**, entry 16), catalyst recycling 5 times without any obviously deactivation. Another base-free system using series of mono- and bimetallic Au-, Pd-, and Pt-based catalysts were reported by Choudhary and Ebitani [79]; bimetallic catalysts were found to be superior to their monometallic counterparts where Pd<sub>20</sub>Pt<sub>80</sub>-PVP/HT emerged as the most efficient heterogeneous catalyst for HMF oxidation to FDCA in  $\geq 99\%$  yield (**Table 2**, entry 17). Another bimetallic catalyst Ni-Pd afforded 100% HMF conversion and 86% FDCA yield-(**Table 2**, entry 18). The presence of Ni help transfer the electronic charge to Pd center,

which makes Pd more electron rich and facilitated the adsorption of more O<sub>2</sub> on the surface of Pd, thus enhancing the catalytic performance and stability. The conversion from fructose to FDCA has also been investigated under optimum condition, 22% FDCA selectivity was discerned with no obvious catalyst deactivation in 6 catalytic runs. The low cost and high performance of bimetallic Ni-Pd system no doubt broadens the perceptions towards Pd catalyst applications in biomass based transformation [80].

The possible mechanism for Pd-catalyzed aerobic oxidation of HMF is like Au as shown in Scheme 6 with HMFCFA being the main intermediate for oxidation to FDCA. The aldehyde group undergoes reversible hydration to form the geminal diol intermediate (**Scheme 4**, steps 1), followed by dehydrogenation of geminal diol on the surface of Pd<sup>2+</sup> species *via* formyl to carboxylic group; the Pd<sup>2+</sup> species serving as an electron acceptor (**Scheme 4**, steps 2). The metallic Pd<sup>0</sup> sites are generally responsible for activation of adsorbed oxygen to the formation of new hydroxide ions (**Scheme 4**, step 6). The oxidation of hydroxyl group of HMFCFA into aldehyde group of FFCA is the rate-determining step and the formation of Pd alcoholate species *via* Pd-hydride shift with the aid of Pd<sup>2+</sup> and OH<sup>-</sup> can accelerate this process (**Scheme 4**, steps 3) [71]. Furthermore, the repeat of step 2 will generate geminal diol intermediate that ensue FDCA.

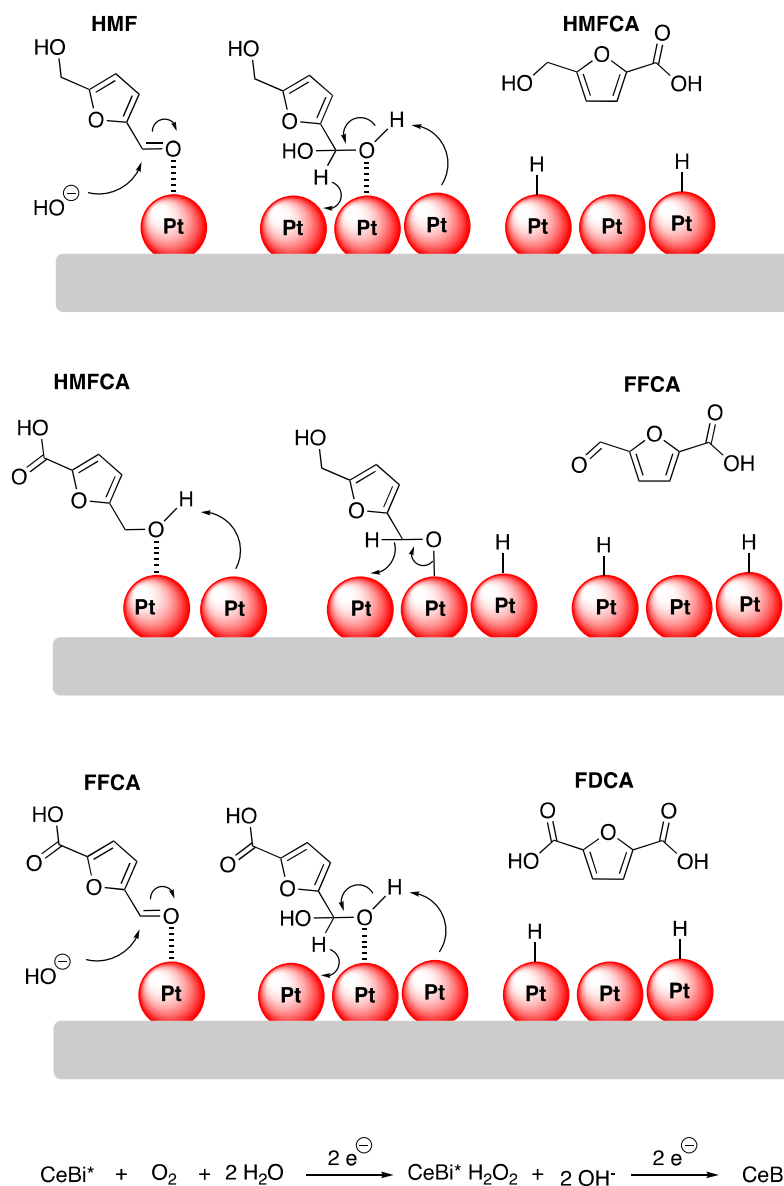


**Scheme 4.** Aerobic oxidation of HMF into FDCA over Pd catalyst.

### 2.1.3. Platinum (Pt)

Platinum (Pt) based catalysts has been disclosed for the activation for HMF oxidation reaction, among the other noble metal catalysts [81,82]. Pt/C was a good catalyst candidate for HMF oxidation to FDCA [83]. Verdeguer et al. focused on Pt/C under normal reaction condition (1.25 M NaOH solution, 25 °C, with O<sub>2</sub> flow rate at 2.5 mL s<sup>-1</sup>), which resulted in 100% HMF conversion and 81% FDCA yield [84]. Bi was found to have a positive effect for Pt/C catalytic system on the HMF oxidation to FDCA (**Table 3**, entries 1 and 2) as under the optimum condition, Pt/C gave only 69% yield of FDCA, while Pt-Bi/C could dramatically increase that yield to 99% [85]. Additionally, the addition of Bi could also improve the stability of the catalyst. Furthermore, the same research group observed the superior of Bi activity and stability when compared Pt/TiO<sub>2</sub> with Pt-Bi/TiO<sub>2</sub> (**Table 3**, entries 3 and 4) under the same reaction condition; FDCA yield increased from 84% to 99% [86]. Miao et al. also

found that the addition of Bi to the CeO<sub>2</sub> support could greatly improve the catalytic performance of Pt/CeO<sub>2</sub>; Pt/Ce<sub>0.8</sub>Bi<sub>0.2</sub>O<sub>2-δ</sub> afforded 100% HMF conversion and 98% yield of FDCA, while HMF conversion was less than 20% over Pt/CeO<sub>2</sub> catalyst (**Table 3**, entries 5 and 6) [87,88]. The mechanism among Bi and Ce-catalyzed reaction garnered interest. The first step entailed Pt-alkoxide intermediate formation under alkaline condition, hydroxide ion through nucleophilic attack. H-Elimination was achieved when hydroxide intermediate captured the hydride which transferred to aldehyde groups, with concomitant release of metallic Pt and two electrons. Furthermore, the aldehyde group was changed to carboxylic group (**Scheme 5a-c**). The intermediate geminol diol generated under alkaline condition and being on the surface of Pt<sup>2+</sup> species, underwent dehydrogenation to carboxylic group and deposited two electrons. The electrons then transferred O<sub>2</sub> and water to CeBi peroxide intermediate, which upon dissociation formed new hydroxide ion. Ce-based catalyst afforded oxygen vacancy accompanied by Bi (**Scheme 5d**). The oxygen reduction process could not occur, because CeO<sub>2</sub> showed a lower redox activity at low temperature with a small amount of oxygen vacancies. Concurrently, Bi accelerated the dissociation of the O–O bond of the formed peroxide intermediates.



**Scheme 5.** The proposed reaction mechanism for the oxidation of HMF with CeBi\* representing the oxygen vacancy accompanied with the bismuth.

Another Pt-CeO<sub>2</sub> catalyst with nitrogen-doped-carbon-decorated (Pt/NC-CeO<sub>2</sub>) was reported by Ke et al. for the aerobic oxidation of HMF [89]. Under homogeneous base conditions, 99% FDCA yield was attained (**Table 3**, entry 7), the impressive results were attributed to the abundant surface defects, enhanced surface basicity, and favorable electron-deficiency; new catalyst showed good stability and reusability. Another nitrogen-doped carbon-based protocol was described using ethylenediamine (EDA) as nitrogen source (Pt/C-

EDA-4.1) which afforded 96% FDCA yield (**Table 3**, entry 8). The introduction of N element introduced the basic site on catalyst surface, specially, the pyridine-type nitrogen with basicity of N-6 site showed higher FDCA selectivity performance than graphene-type nitrogen (N-Q), or pyrrole-type nitrogen (N-5) [90].

**Table 3**

The oxidation of HMF to FDCA over Pt-based catalyst.

Entry	Catalyst	HMF/metal molar ratio	Oxidant	Base [eq.]	T [°C]	Time [h]	Conv (HMF) [%]	Yield (FDCA) [%]	Ref.
1	Pt/C	100	air (40 bar)	Na <sub>2</sub> CO <sub>3</sub> (2 eq)	100	6	100	69	[85]
2	Pt-Bi/C	100	air (40 bar)	Na <sub>2</sub> CO <sub>3</sub> (2 eq)	100	6	100	99	[85]
3	Pt/TiO <sub>2</sub>	100	air (40 bar)	Na <sub>2</sub> CO <sub>3</sub> (2 eq)	100	6	99	84	[86]
4	Pt-Bi/TiO <sub>2</sub>	100	air (40 bar)	Na <sub>2</sub> CO <sub>3</sub> (2 eq)	100	6	99	99	[86]
5	Pt/CeO <sub>2</sub>	200	O <sub>2</sub> (10 bar)	NaOH (4 eq)	23	0.5	100	20	[87]
6	Pt/Ce <sub>0.8</sub> Bi <sub>0.2</sub> O <sub>2-δ</sub>	200	O <sub>2</sub> (10 bar)	NaOH (4 eq)	23	0.5	100	98	[87]
7	Pt/NC-CeO <sub>2</sub>	163	O <sub>2</sub> (4 bar)	Base free	150	4	100	99	[89]
8	Pt/C-EDA-4.1	50	O <sub>2</sub> (10 bar)	Base free	110	12	100	96	[90]
9	Pt/RGO	40	O <sub>2</sub> (50 mL min <sup>-1</sup> )	NaOH (5 eq)	25	24	100	84	[91]
10	Pt/CNT	200	O <sub>2</sub> (30 bar)	Base free	100	12	100	97	[92]

11	Pt/CNTs	100	O <sub>2</sub> (5 bar)	Base free	95	14	100	98	[93]
12	Pt/Al <sub>2</sub> O <sub>3</sub>	100	O <sub>2</sub> (5 bar)	Base free	95	14	94	26	[93]
13	Pt/ $\alpha$ -Al <sub>2</sub> O <sub>3</sub>	43	O <sub>2</sub> (1 bar)	Na <sub>2</sub> CO <sub>3</sub> (1 eq)	140	12	96	96	[87]
14	Pt/ZrO <sub>2</sub>	100	O <sub>2</sub> (5 bar)	Base free	95	14	81	8	[93]
15	Pt/ZrO <sub>2</sub> -ALD-30	70	O <sub>2</sub> (4 bar)	Base free	100	12	100	97	[97]
16	Pt/HT	100	O <sub>2</sub> (5 bar)	Base free	95	14	100	97	[93]
17	Pt/GO	100	O <sub>2</sub> (5 bar)	Base free	95	14	100	95	[93]
18	Pt/PVP-ACS-800	125	O <sub>2</sub> (10 bar)	Base free	110	5	100	100	[95]
19	Pt/C-O-Mg	50	O <sub>2</sub> (10 bar)	Base free	110	12	100	97	[96]
20	CeCP@Pt	5000	O <sub>2</sub> (30 mL min <sup>-1</sup> )	NaOH (2 eq)	70	12	100	96	[97]
21	110-Fe <sub>3</sub> O <sub>4</sub> @C@Pt	24	O <sub>2</sub> (100 mL min <sup>-1</sup> )	Na <sub>2</sub> CO <sub>3</sub> (2 eq)	90	4	100	100	[98]

---

Carbon-based supports namely activated carbon,–reduced graphene oxide (RGO) and carbon nanotubes (CNT) as matrixes to support Pt has attracted tremendous attention in recent years with adequate coverage on the underlying, reaction parameters and synergistic effect of Pt for HMF oxidation process [99]. Carbon-based supports can afford not only a large number of acidic sites and basic sites together with numerous functional groups, but due to its relatively stable physical properties, render them a good candidate for HMF oxidation to FDCA. As an example, Pt/RGO was prepared using ethylene glycol reduction [91], that afforded quantitative HMF conversion and 84% FDCA yield at room temperature in 24 h (**Table 3**, entry 9) and could be recycled three times without obvious deactivation; HMFCAs being a major intermediate during the catalytic process. Pt/CNT, Pd/CNT, Ru/CNT were synthesized under base-free conditions to investigate the oxidation of HMF to FDCA where Pt/CNT displayed the highest selectivity and activity towards FDCA formation with complete HMF conversion and 97% FDCA yield (**Table 3**, entry 10) [92]. The functional groups on the surface of CNT enhanced the adsorption of HMF as well as the reaction intermediates; carbonyl/quinone and phenol played an important role in FDCA formation [100]. Additionally,  $sp^2$  network of CNT facilitated the desorption of FDCA, thus enhancing the catalytic performance for FDCA selectivity and yield. After 5 cycles, the selectivity for FDCA and the yield decreased marginally, which showed the stability of catalyst. Similar results were reported by Zhou et al. using Pt/CNT [93], where FDCA yield attained was 98%, with complete HMF conversion under mild conditions (**Table 3**, entry 11). The data presented in entries 11, 12, 14, 16 and 17 (**Table 3**) was obtained under the same reaction conditions (HMF/Pt=100, 5 bar  $O_2$ , base free, 95 °C, 14 h) which affirms that Pt loaded on carbon-based supports exhibited better performance (Pt/CNTs, Pt/GO yielded FDCA 98% and 95% in entries 11 and 17) than loaded on typical metal oxide (Pt/ $Al_2O_3$ , Pt/ $ZrO_2$  yielded FDCA 26%

and 8% in entries 12 and 14); notably, Pt/HT could also attain 97% FDCA yield (**Table 3**, entry 16) but had a problem of poor catalyst recycling due to the leaching of solid base in an aqueous solution. Sahu et al. [88] reported that by decreasing HMF/Pt molar ratio from 100 to 43 and increasing the reaction temperature from 94 °C to 140 °C, and by deploying homogeneous base Pt/ $\alpha$ -Al<sub>2</sub>O<sub>3</sub> catalyst, FDCA yield could be increased from 26% to 96% (**Table 3**, entry 12 vs. 13). Pt/ZrO<sub>2</sub> also improved the catalytic performance through catalyst synthesis processes. In comparison with Pt/ZrO<sub>2</sub>, Pt/ZrO<sub>2</sub>-ALD-x (atomic layer deposition x refers to the number of deposition cycles) [93,94] enhanced the FDCA yield from 8% to 97% (**Table 3**, entry 14 vs. 15); striking improvement was attributed to the homogeneous dispersion of the Pt nanoparticles and high dispersion of active sites and the higher C=O adsorption properties.

Another interesting porous carbon-based support was prepared by the carbonization of chitosan with K<sub>2</sub>CO<sub>3</sub> at 600-800 °C and were adorned with PVP-capped Pt nanoparticles; improved active sites resulted in 100% HMF conversion and 100% FDCA yield under base-free conditions (**Table 3**, entry 18), and displayed good stability over five cycles without significant deactivation. Furthermore, Pt/C-O-Mg secured by coating MgO particles with resorcinol carbonation at 800 °C was used as catalyst towards HMF oxidation under base-free conditions [96], 97% FDCA obtained (**Table 3**, entry 19); surface of catalyst support being alkaline due to the formation of a C-O-Mg bond. Notably, further scaling up of the reaction for 4 and 20 times afforded 75% isolated yield of FDCA with high purity (99.5%) thus making it a good candidate for industrial application.

Cerium coordination polymer (CeCP) synthesized with 1,3,5-benzenetricarboxylic as the ligand for a new catalyst CeCP@Pt was revealed by Gong et al. [97] which afforded 96% yield of FDCA under optimum conditions (**Table 3**, entry 20); besides nearly quantitative HMF conversion capacity (HMF/Pt=5000 mole ratio),—as a robust catalyst, it could be

recycled five times with no apparent catalyst deactivation.

Last but not least, a magnetic Fe<sub>3</sub>O<sub>4</sub>@C@Pt, which comprised a core-shell Fe<sub>3</sub>O<sub>4</sub> with amorphous carbon as matrix to support Pt, was reported by Zhang [98] with three different variants of 90-Fe<sub>3</sub>O<sub>4</sub>@C@Pt, 100-Fe<sub>3</sub>O<sub>4</sub>@C@Pt and 110-Fe<sub>3</sub>O<sub>4</sub>@C@Pt. Under optimum conditions, 110-Fe<sub>3</sub>O<sub>4</sub>@C@Pt attained 100% FDCA yield after 4 h (**Table 3**, entry 21). The impressive catalytic performance was ascribed to the high reflux temperature, thus leading to high degree of crystallization; 110-Fe<sub>3</sub>O<sub>4</sub>@C@Pt with well-crystallized Pt nanoparticle clusters and unique islet morphology enhanced the yield of FDCA than the other two catalysts.

#### 2.1.4. Ruthenium (Ru)

Ru has attracted more interest because of its impressive activity attained at a reasonable cost; price of Ru is ~ 4% of Au and Pt costs per gram [101]. Carbon-based supported Ru have been predominantly investigated as illustrated by Yi et al. [102] who used Ru/C as catalyst using different kind of base in dilute substrate solution (HMF/Ru=0.02); various bases were screened ranging from strong base to weak base like NaOH, K<sub>2</sub>CO<sub>3</sub>, Na<sub>2</sub>CO<sub>3</sub> when full HMF conversion occurred and the yield of FDCA increased from 69%, 80% to 93%. The study indicated that strong alkaline environment favors the degradation or condensation of HMF. Notably, the deployment of 1 eq. CaCO<sub>3</sub> under optimum conditions, offered 95% FDCA yield (**Table 4**, entry 1). Interesting, in dilute substrate concentration (HMF/Ru=0.01) and prolonged reaction time to 10 h under base-free conditions, 88% FDCA yield could be attained (**Table 4**, entry 2). Chen et al. [103] discussed Ru/C as catalyst with aqueous H<sub>2</sub>O<sub>2</sub> as oxidant obtaining 91% FDCA yield after 6 h (**Table 4**, entry 3). Kerdi et al. [104] achieved 75% FDCA yield under 40 bar of air pressure with a relative high HMF concentration (HMF/Ru=100). Xie et al. reported the use of Ru/C in toluene which provided 95% yield of

DFF [105], Ru being superior to Pt, Pd, Rh and Au in attaining higher DFF selectivity. The same research group [106] using 0.5 eq (HT) as base obtained 78% FDCA yield (**Table 4**, entry 5). Zheng et al. [107] disclosed that Ru/C with 4.3 eq. Mg(OH)<sub>2</sub> for an impressive 97% FDCA yield at 108 °C in 8 h under 10 bar of O<sub>2</sub> (**Table 4**, entry 6). ZrO<sub>2</sub>, TiO<sub>2</sub> and Al<sub>2</sub>O<sub>3</sub> have been reported for alcohol oxidation reaction [108], under the same optimum condition with Ru/C (**Table 4**, entries 6 to 9); FDCA yield (82-86%) were lower than attained using active carbon (FDCA yield 97%) despite lower HMF loading from 40 to 30.–Furthermore, ZrO<sub>2</sub>, TiO<sub>2</sub> and Al<sub>2</sub>O<sub>3</sub> led to a lower carbon balance than active carbon (86-88% vs 97%) possibly due to the favorable formation of unidentified degradation or polymerization of HMF than inert carbon [109]. Water apparently is an ideal solvent for HMF oxidation to FDCA [27] and not surprisingly, most of aforementioned HMF oxidations used water as a solvent. Recently, Liu et al. explored the use of DMSO/H<sub>2</sub>O solvent system with commercial Ru/C to attain 93% FDCA yield (**Table 4**, entry 10) [110].–Besides, 65% FDCA yield could be achieved from concentrated fructose solution through a two-step process, when compared to pure H<sub>2</sub>O and DMSO solution; HMF was more stable in DMSO/H<sub>2</sub>O solvent system in an alkaline medium. These finding are suggestive of lowering the cost of FDCA synthesis process which bodes well for a large industrial scale up production. Such comparative analysis, from entry 1 to 10 in **Table 4**, indicated that inert activate carbon is a preferable support for HMF oxidation reaction which may broaden the perspective of its application in intensified processes.

**Table 4**

The oxidation of HMF to FDCA over Ru based catalyst.

Entry	Catalyst	HMF/metal molar ratio	Oxidant	Base [eq.]	T [°C]	Time [h]	Conv (HMF) [%]	Yield (FDCA) [%]	Ref.
1	Ru/C	0.02	O <sub>2</sub> (2 bar)	CaCO <sub>3</sub> (1 eq)	120	5	100	95	[102]
2	Ru/C	0.01	O <sub>2</sub> (2 bar)	Base free	120	10	100	88	[102]
3	Ru/C	10	H <sub>2</sub> O <sub>2</sub> (35 wt %)	Na <sub>2</sub> CO <sub>3</sub> (1 eq)	75	6	100	91	[103]
4	Ru/C	100	Air (40 bar)	NaHCO <sub>3</sub> (4 eq)	100	2	100	75	[104]
5	Ru/C	80	O <sub>2</sub> (20 bar)	HT (0.5 eq)	140	0.3	100	78	[106]
6.	Ru/C	40	O <sub>2</sub> (10 bar)	Mg(OH) <sub>2</sub> (4.3 eq)	108	8	100	97	[107]
7.	Ru/ZrO <sub>2</sub>	30	O <sub>2</sub> (10 bar)	Mg(OH) <sub>2</sub> (4.3 eq)	108	8	100	82	[107]
8.	Ru/TiO <sub>2</sub>	30	O <sub>2</sub> (10 bar)	Mg(OH) <sub>2</sub> (4.3 eq)	108	8	100	80	[107]
9	Ru/Al <sub>2</sub> O <sub>3</sub>	30	O <sub>2</sub> (10 bar)	Mg(OH) <sub>2</sub> (4.3 eq)	108	8	100	86	[107]
10.	Ru/C	42.8	O <sub>2</sub> (40 bar)	NaHCO <sub>3</sub> (2 eq)	130	12	100	93	[110]

11.	Ru/K-OMS-2	63	O <sub>2</sub> (20 bar)	NaOH (4 eq)	120	6	100	93	[111]
12.	Ru/CTFs	40	air (20 bar)	Base free	140	3	99	78	[112]
13.	Ru/ZrO <sub>2</sub> -H-aero	31	O <sub>2</sub> (10 bar)	Base free	120	16	100	97	[113]
14.	Ru/HAP	25	O <sub>2</sub> (10 bar)	Base free	120	24	100	99	[114]
15	Ru/MnCo <sub>2</sub> O <sub>4</sub>	33	Air (24 bar)	Base free	120	10	100	99	[115]
16	Ru/Mn <sub>6</sub> Ce <sub>1</sub> O <sub>y</sub>	80	O <sub>2</sub> (10 bar)	Base free	150	15	100	99	[116]
17	Ru(OH) <sub>x</sub> /MgO	20	O <sub>2</sub> (2.5 bar)	Base free	140	20	100	100	[117]
18	Ru(OH) <sub>x</sub> /HT	20	O <sub>2</sub> (2.5 bar)	Base free	140	20	100	100	[117]
19	Ru(OH) <sub>x</sub> /MgAl <sub>2</sub> O <sub>4</sub>	20	O <sub>2</sub> (2.5 bar)	Base free	140	42	100	60	[128]
20	Ru(OH) <sub>x</sub> /TiO <sub>2</sub>	20	O <sub>2</sub> (2.5 bar)	Base free	140	6	78	22	[118]
21	Ru(OH) <sub>x</sub> /Al <sub>2</sub> O <sub>3</sub>	20	O <sub>2</sub> (2.5 bar)	Base free	140	6	100	30	[118]
22	Ru(OH) <sub>x</sub> /ZrO <sub>2</sub>	20	O <sub>2</sub> (2.5 bar)	Base free	140	6	90	38	[118]
23	Ru(OH) <sub>x</sub> /CeO <sub>2</sub>	20	O <sub>2</sub> (2.5 bar)	Base free	140	6	100	40	[118]
24	Ru(OH) <sub>x</sub> /Fe <sub>3</sub> O <sub>4</sub>	20	O <sub>2</sub> (2.5 bar)	Base free	140	6	100	50	[118]
25	Ru(OH) <sub>x</sub> /La <sub>2</sub> O <sub>3</sub>	22	O <sub>2</sub> (30 bar)	Base free	100	5	98	48	[119]

---

A novel basic support K-OMS-2 (K-exchanged octahedral molecular sieve-2) as matrix to adorn Ru was explored by Lucas et al. [111] which attained 93% FDCA yield under optimum conditions (**Table 4**, entry 11); the basicity of K-OMS-2 was inadequate.

Ru-based catalyst under base-free condition has been widely investigated as Ru clusters supported on covalent triazine frameworks (CTFs) were discussed by Artz and Palkovits [112]; mesoporous CTFs (37% FDCA yield) showed better catalytic performance than microporous-version of CTFs (8.2% FDCA yield) in catalyst screening. Thus, porosity, specific area, and hydrophilicity of the solid support influenced the catalytic performance when 78% FDCA yield was obtained under optimum conditions (**Table 4**, entry 12) with good recyclability exhibited by Ru/CTFs. Pichler et al. [113] studied Ru supported on ZrO<sub>2</sub> in depth with three variations of the synthesized support: ZrO<sub>2</sub>-H-aero, ZrO<sub>2</sub>-H-SBA, ZrO<sub>2</sub>-soft and two commercial ZrO<sub>2</sub>-C-mono, ZrO<sub>2</sub>-C-tet. Ru/ZrO<sub>2</sub>-H-aero showed the highest activation with 97% FDCA yield (**Table 4**, entry 13); which attributed to the higher surface area and smaller Ru nanoparticles size than the others. However, the catalyst suffers from the significant deactivation upon recycling. Ru supported on hydroxyapatite has been reported [114], which afforded 99% FDCA (**Table 4**, entry 14) while Ru/MnCo<sub>2</sub>O<sub>4</sub> [115] gave 99% FDCA yield (**Table 4**, entry 15). The impressive results were attributed to the Lewis and Brønsted acidic active sites on the surface of support which enhanced the catalytic performance; synergetic effect between Ru and Mn, Co directed the reaction *via* the formation of DFF and FFCA formation rather than through HMFCa to FDCA and the catalyst reusability showed five successive runs without obvious deactivation. MnO<sub>x</sub>-CeO<sub>2</sub> composite displayed excellent performance for HMF oxidation with 91% FDCA yield under 20 bar O<sub>2</sub> pressure and homogeneous basic conditions [120]. A modification of Ru/Mn<sub>6</sub>Ce<sub>1</sub>O<sub>y</sub> as a catalyst was reported by Gao et al. [116] wherein an exceptional 99% FDCA yield was

achieved in 15 h with higher HMF/Ru mole ratio (80) (**Table 4**, entry 16); synergistic effect between Mn and Ce and higher surface concentration no doubt increased the available and mobility of active oxygen species thus enhancing the catalytic activity.

Ru(OH)<sub>x</sub> as active sites showed selective aerobic oxidation of aromatic and aliphatic alcohol to aldehydes and ketones [121-123] and Ru(OH)<sub>x</sub> supported on three different types of Mg-based carrier materials (MgO, HT or MgAl<sub>2</sub>O<sub>4</sub>) was examined for HMF oxidation to FDCA (**Table 4**, entries 17, 18 and 19); Ru(OH)<sub>x</sub>/MgO and Ru(OH)<sub>x</sub>/HT afforded 100% FDCA yield under optimum conditions. ICP analysis confirmed the presence of 26% and 38% Mg ions in HT and MgO post-reaction solution, respectively, corresponding to high pH alkaline environment that favored the FDCA formation. In contrast, Ru(OH)<sub>x</sub>/MgAl<sub>2</sub>O<sub>4</sub> delivered 60% FDCA yield after 42 h when 35% formic acid was observed. The formation of HMFCa was found to be rate-limiting step. Furthermore, to avoid Mg ions leaching, the same group employed diverse metal oxide supports (TiO<sub>2</sub>, Al<sub>2</sub>O<sub>3</sub>, ZrO<sub>2</sub>, CeO<sub>2</sub> and Fe<sub>3</sub>O<sub>4</sub>) as carriers to support Ru(OH)<sub>x</sub> (**Table 4**, entries 20-24), all of them under base-free condition, the yield of FDCA was lower than 50%. Ru(OH)<sub>x</sub>/Al<sub>2</sub>O<sub>3</sub> and Ru(OH)<sub>x</sub>/ZrO<sub>2</sub> induced the formation of formic acid. Ru(OH)<sub>x</sub>/Fe<sub>3</sub>O<sub>4</sub> displayed the highest selectivity for FDCA formation, however, the formation of humins was still approximately 30%. Ru(OH)<sub>x</sub>/CeO<sub>2</sub> could increase the yield of FDCA from 40% to 60% up on prolongation of the reaction time to 16 h. Later, the same group evaluated these catalyst in ionic liquid, the highest performance was discerned for Ru(OH)<sub>x</sub>/La<sub>2</sub>O<sub>3</sub> when [EMIm][OAc] was employed as solvent at 30 bar O<sub>2</sub>, 100 °C during 5 h, 48% FDCA yield and 12% HMFCa was attained (**Table 4**, entry 25).

Trimetallic catalyst ZnFe<sub>1.65</sub>Ru<sub>0.35</sub>O<sub>4</sub> [124] was synthesized for HMF oxidation, which gave the maximum FDCA yield of 91.2% at 130 °C during 16 h in H<sub>2</sub>O/DMSO (1:2, v/v). Furthermore, when ZnFe<sub>1.65</sub>Ru<sub>0.35</sub>O<sub>4</sub> was employed to oxidize HMF (obtained through fructose dehydration process), 70.5% FDCA yield was obtained under optimum conditions.

### **2.1.5. Silver (Ag)**

Ag, another important noble metal, was explored initially for HMF oxidation in 1953; Ag<sub>2</sub>O oxidized HMF to HMFCAs with high selectivity [125-127]. Homogeneous Ag(I)-catalyzed a wide range of aliphatic and aromatic aldehydes in water with oxygen as an oxidant to corresponding carboxylic acids quantitatively [128], which indicated Ag could be used as an excellent candidate for HMF oxidation reaction.

**Table 5**

Oxidation of HMF-over Ag-based catalyst.

Entry	Catalyst	HMF/meta 1 molar ratio	Oxidant	Base [eq.]	T [°C]	Time [h]	Conv (HMF) [%]	Yield (DFF) [%]	Yield (HMFCFA) [%]	Yield (FDCA) [%]	Ref.
1	Ag/ZrO <sub>2</sub>	100	Air (10 bar)	NaOH (4 eq)	100	5	100	--	92	5	[55]
2	Ag/TiO <sub>2</sub>	100	Air (10 bar)	NaOH (4 eq)	100	5	100	--	14	3	[55]
3	Ag/CeO <sub>2</sub>	100	Air (10 bar)	NaOH (4 eq)	100	5	100	--	74	3	[55]
4	Ag/MgO	100	Air (10 bar)	NaOH (4 eq)	100	5	100	--	60	1	[55]
5	Ag-PVP/ZrO <sub>2</sub> (1:1)	130	O <sub>2</sub> (60 mL min <sup>-1</sup> )	NaOH (4 eq)	20	2	100	--	98	--	[129]
6	Ag-OMS-2	6	Air (15 bar)	Base free	165	4	99	99	0	0	[130]
7	Ag <sub>2</sub> O	2	H <sub>2</sub> O <sub>2</sub>	Na <sub>2</sub> CO <sub>3</sub> (4 eq)	90	1	100	--	98	0	[131]

Insights into metal and supports for catalytic HMF oxidation, Au/ZrO<sub>2</sub>, Ag/ZrO<sub>2</sub> as well as other supports TiO<sub>2</sub>, CeO<sub>2</sub>, MgO were examined [55]. Ag/ZrO<sub>2</sub> catalyst demonstrated exclusively highest HMFCFA yield ( $\geq 92\%$ ) under the identical optimized conditions (**Table 5**, entry 1) when compared to other supports TiO<sub>2</sub>, CeO<sub>2</sub> and MgO (**Table 5**, entries 2, 3, 4), while Au/ZrO<sub>2</sub> afforded high FDCA selectivity (**Table 1**, entry 22). Furthermore, poly(vinylpyrrolidone) (PVP) stabilized AgNPs supported on ZrO<sub>2</sub> was optimized in terms of base types, the size of Ag particle as well as Ag loading for HMF oxidation. Comparison among no PVP capped catalyst in the synthesis process-Ag/ZrO<sub>2</sub>, 2.5% Ag-PVP/ZrO<sub>2</sub>(1:1) showed displayed higher efficiency, 98.2% HMFCFA yield obtained in room temperature in 2 h (**Table 5**, entry 5), the weak interaction between Ag NPs and ZrO<sub>2</sub> contributed to high HMFCFA selectivity [129]. Another study uncovered that Ag-OMS-2 (octahedral molecular sieve) as catalyst, K-OMS-2 being a mixture of valence forms of manganese (Mn<sup>2+</sup>, Mn<sup>3+</sup> and Mn<sup>4+</sup>), makes it a good redox type support for HMF oxidation [130]. Furthermore, the incorporation of Ag improved the activity of the catalyst which afforded 99% DFF yield under base-free conditions (**Table 5**, entry 6). Our own investigations with Ag<sub>2</sub>O in aqueous H<sub>2</sub>O<sub>2</sub> as oxidant for HMFCFA production, under optimum condition (90 °C, 4 eq. Na<sub>2</sub>CO<sub>3</sub> in 1 h) afforded 98% HMFCFA yield (**Table 5**, entry 7) [131]. During the catalytic process, Ag<sup>+</sup> was reduced to Ag<sup>0</sup> while at the same time aldehyde group oxidized to carboxylic group, and the addition of H<sub>2</sub>O<sub>2</sub> closed the catalyst cycle, oxidizing Ag<sup>0</sup> to Ag<sup>+</sup> thus motivating the reaction further. MW-assisted reaction shortened the reaction time, thus increasing productivity. These investigations with Ag no doubt paved the way for the selective oxidation of HMF to high value intermediates, like HMFCFA.

## 2.2. Non-noble metal-based catalyst

It is well known that the cost of noble metal catalyst restricts their practical application in the production of FDCA. Consequently, research focus has shifted to non-noble metal catalysts for HMF oxidation from the economical point of view; predominantly, Mn, Co, Cu, Fe, Mo and V were studied in more detail.

### 2.2.1. Manganese (Mn)

Among non-noble metal catalysts, Mn-based catalysts were widely investigated toward oxidation reaction, owing to their variety of oxidation states, ease of oxygen absorption, reduction as well as higher storage capacity [132]. Based on this premise, it is meaningful to develop an economical and greener Mn-based catalyst for HMF oxidation producing FDCA or other high value compounds like DFF, HMFCFA and FFCA.

Hayashi et al. reported the use of MnO<sub>2</sub> [133] with 3 eq. NaHCO<sub>3</sub> under 10 bar O<sub>2</sub>, 120 °C, 24 h for oxidation and obtained 95% FDCA yield (**Table 6**, entry 1); MnO<sub>2</sub>-NaHCO<sub>3</sub> catalytic system can also convert furfural and furfuryl alcohol to furfuryl carboxylic acid with 99% and 95% yield, respectively and MnO<sub>2</sub> can be easily recycled 3 times with no apparent deactivation by calcination 300 °C in air. The same group [134] delineated that MnO<sub>2</sub> crystal structure plays an important role in HMF oxidation to FDCA. The relationship between structure and activity for six types of crystalline MnO<sub>2</sub> ( $\alpha$ -,  $\beta$ -,  $\gamma$ -,  $\delta$ -,  $\epsilon$ -, and  $\lambda$ -MnO<sub>2</sub>) were investigated in depth which showed that the vacancy formation energies at  $\beta$ -MnO<sub>2</sub> was lowest than the others for the abundant planar oxygen sites, which renders it a good candidate for HMF oxidation; 91% yield of FDCA could be obtained under optimum conditions (**Table 6**, entry 2). Additionally, the conversion of FFCA to FDCA was found to be the rate-limiting step, and the catalytic performance can be improved through increase the area surface of  $\beta$ -MnO<sub>2</sub>.

**Table 6**

HMF oxidation over Mn-based catalyst.

Entry	Catalyst	Oxidant	Base [eq.]	T	Time	Conc.	Yield	Yield	Yield	Yield	Ref.
				[°C]	[h]	(HMF)	(DFP)	(HMFCFA)	(FFCA)	(FDCA)	
						[%]	[%]	[%]	[%]	[%]	
1	MnO <sub>2</sub>	O <sub>2</sub> (10 bar)	NaHCO <sub>3</sub> (3 eq)	120	24	100	0	0	0	95	[133]
2	MnO <sub>2</sub>	O <sub>2</sub> (10 bar)	NaHCO <sub>3</sub> (3 eq)	100	24	100	0	0	0	91	[134]
3	MC-6	O <sub>2</sub> (20 bar)	KHCO <sub>3</sub> (4 eq)	75	15	98	0	0	1	91	[135]
4	Mn <sub>0.75</sub> Fe <sub>0.25</sub>	O <sub>2</sub> (8 bar)	NaOH (4 eq)	90	24	79	0	0	69	9	[136]
5	MnFe <sub>2</sub> O <sub>4</sub>	TBHP	Base free	100	5	--	--	--	--	85	[137]

Mn-based bimetallic catalyst showed impressive performance as exemplified by-MnO<sub>x</sub>-CeO<sub>2</sub> composite for the oxidation of HMF [135]. Compared with mono MnO<sub>2</sub> as catalyst, Ce<sup>3+</sup> and Mn<sup>4+</sup> displayed synergistic interaction, where Mn<sup>4+</sup> ions were the active sites and the lattice oxygen transfer from CeO<sub>2</sub> to MnO<sub>x</sub> enhanced the catalytic performance under mild condition; 91% yield of FDCA could be obtained with MnO<sub>x</sub>-CeO<sub>2</sub>(Mn/Ce=6) under optimum conditions (**Table 6**, entry 3) with recyclability up to five times without deactivation. Neatu et al. reported Mn<sub>0.75</sub>/Fe<sub>0.25</sub> composite as catalyst for one-pot oxidation of HMF to FDCA (**Table 6**, entry 4) when only 9% FDCA was obtained, the major intermediate being FFCA in 69% yield [136]. Furthermore, in the absence of catalyst under 8 eq. NaOH and 8 bar O<sub>2</sub>, 87% FFCA yield was attained in half an hour. Acidification and filtration of FFCA then oxidation with Mn<sub>0.75</sub>Fe<sub>0.25</sub> as catalyst afforded ~ 90% FDCA yield in a new reaction system (0.05 g of catalyst, 2 mmol NaOH, 8 bar O<sub>2</sub> for 24 h at 90 °C). Various magnetic ferrites catalyst such as CuFe<sub>2</sub>O<sub>4</sub>, CoFe<sub>2</sub>O<sub>4</sub>, MnFe<sub>2</sub>O<sub>4</sub>, MgFe<sub>2</sub>O<sub>4</sub> and Fe<sub>3</sub>O<sub>4</sub> have been screened for the oxidation of HMF [137]; MnFe<sub>2</sub>O<sub>4</sub> displayed the highest activation, and 85% FDCA yield could be obtained using TBHP as an oxidant under base-free conditions (**Table 6**, entry 5). The better performance was due to the variable oxidation state of Mn and the synergetic effect between Mn and Fe<sub>2</sub>O<sub>4</sub>; magnetic property facilitated the easy recovery and reuse up to—four times without noticeable deactivation. Other Mn-based bimetallics such as Fe<sub>3</sub>O<sub>4</sub>/Mn<sub>3</sub>O<sub>4</sub>, Mn<sub>0.7</sub>Cu<sub>0.05</sub>Al<sub>0.25</sub> and octahedral MnO<sub>2</sub> molecular sieve exhibited high efficient for DFF selectivity [138-140]. These studies have shown that Mn can be used for the oxidation of HMF because of active sites or support and deserve further investigations and application in the future.

### 2.2.2. Cobalt (Co)

Homogeneous Co-based catalyst namely, Co/Mn/Br [141], [Co(OAc)<sub>2</sub>/Zn(OAc)<sub>2</sub>/NaBr] [142] and [Co(OAc)<sub>2</sub>/Mn(OAc)<sub>2</sub>/NaBr] [143] have been used for the oxidation of 5-HMF oxidation with satisfactory performance. Co-Mn heterogeneous catalysts were identified as excellent candidates. A nanoscale center-hollowed heterogeneous MnCo<sub>3</sub>O<sub>4</sub> synthesized by thermal method exhibited quantitative HMF conversion and 71% FDCA yield under O<sub>2</sub> atmosphere under mild conditions (**Table 7**, entry 1). The lowest reduction peaks by H-TPR improved oxygen mobility thus enhancing the catalytic performance. Another Co-Mn composite mixed oxide with different mole ratio was prepared simply by solid-state grinding method and Co-Mn-0.25 secured 99% HMF conversion and 95% FDCA yield (**Table 7**, entry 2); compared to traditional liquid-state co-precipitation method, a much easier-operation and green preparative method showed ~40% FDCA yield advantage with larger BET area, high lattice oxygen mobility and variety of valence states of Mn contributing to better catalytic performance. Successful recycling 5 times and ICP analysis affirmed its stability as negligible concentration of Mn and Co could be seen in leachate solution. Furthermore, Co encapsulated in graphitic carbon and tailored with Mn and N on lignin complex (Co-Mn/N@C) was reported as catalyst for HMF oxidation to FDCA [144]; 96%-yield of FDCA was obtained (**Table 7**, entry 3). The N-doped carbon as support increased not only the catalyst surface basicity, but also the content of pyridinic N, functioning as electron acceptor for the dispersion of Co NPs, thus contributing to catalytic activation with good stability and recyclability up to six cycles. Another catalyst, Li<sub>2</sub>CoMn<sub>3</sub>O<sub>8</sub>—used urea and citric acid as agents through pyrolysis method and displayed efficient HMF oxidation, 80% isolate FDCA yield obtained in AcOH solution with NaBr as catalyst (**Table 7**, entry 4). Another tri-elemental catalyst Co/Mn/Br (molar ratio 1/0.015/0.5) was reported to afford 90% FDCA from HMF at 180 °C and 30 bar [145], the synergism between Co and Mn facilitated the rapid generation of bromo radicals in three steps. In this regard, the reaction proceeds smoothly

under the complete redox catalytic cycle.

**Table 7**

HMF oxidation over Co-based catalyst.

Entry	Catalyst	Oxidant	Base[eq.]	T [°C]	Time [h]	Conv (HMF) [%]	Yield (DFF) [%]	Yield (HMFCA) [%]	Yield (FFCA) [%]	Yield (FDCA) [%]	Ref.
1	MnCo <sub>2</sub> O <sub>4</sub>	O <sub>2</sub> (10 bar)	KHCO <sub>3</sub> (3 eq)	100	24	100	--	--	--	71	[146]
2	Co-Mn-0.25	O <sub>2</sub> (10 bar)	NaHCO <sub>3</sub> (2 eq)	120	5	99	0	0	0	95	[147]
3	Co-Mn/N@C	O <sub>2</sub> (1 bar)	Na <sub>2</sub> CO <sub>3</sub> (1 eq)	85	12	99	--	1	2	96	[144]
4	Li <sub>2</sub> CoMn <sub>3</sub> O <sub>8</sub>	O <sub>2</sub> (55 bar)	NaBr (0.03 eq)	150	8	100	--	--	--	80	[148]
5	CoxOy-N@C	O <sub>2</sub> (10 bar)	K <sub>2</sub> CO <sub>3</sub> (0.2 eq)	100	6	100	--	1	--	96 <sup>a</sup>	[149]
6	Co-Sac/N@C	O <sub>2</sub> (1 bar)	Na <sub>2</sub> CO <sub>3</sub> (1 eq)	85	8	100	0	0	0	99	[150]
7	Resin-Co-Py	TBHP	Base free	100	24	96	3	--	--	91	[151]

a: yield of FDCAM (2,5-furandicarboxylic acid methyl)

Co supported on variety of carbon-based catalysts have been reported as exemplified by CoxOy-N@C obtained by pyrolyzing the ligand (homogenous Co salt and 1,10-phen after adsorption on active carbon) under N<sub>2</sub> flow at 800 °C [149] and affording 96% yield of FDCAM (2,5-furandicarboxylic acid methyl) (**Table 7**, entry 5). Furthermore, Zhou et al. [150] reported another N-doped carbon supported Co single-atom catalyst (Co-SAs/N@C) for HMF oxidation with 99% FDCA yield (**Table 7**, entry 6). Interestingly, FDCA synthesized *via* C5 route with furfural as starting material with Co-SAs/N@C as catalyst in CO<sub>2</sub> flow gave 86% FA conversion and 72% yield of FDCA with good stability and recyclability. Gao et al. [151] reported Merrifield resin-supported Co(II)-meso-tetra(4-pyridyl)-porphyrin (Merrifield resin-Co-Py) as catalyst in CH<sub>3</sub>CN with *tert*-BOOH as oxidant to afford FDCA in 91% yield at 100 °C during 24 h (**Table 7**, entry 7); DFF was the major intermediate, with no significant loss in six recyclings. Another meaningful research showed that starting from fructose, FDCA was obtainable in one-pot with 72% fructose conversion and 99% FDCA selectivity using Co acetylacetonate encapsulated in sol-gel silica [152]. SiO<sub>2</sub>-gel is suitable for the dehydration of fructose, while Co metal functioned in the HMF oxidation, the cooperative effect of acidic matrix and metal give rise to high selectivity of FDCA.

### 2.2.3. Copper (Cu)

Cu-based homogeneous catalysts were found to be active for DFF production [153-155]. Recently, Ren et al. [156] performed DFT calculation for HMF adsorption on the surface of CuO (111) and Co<sub>3</sub>O<sub>4</sub> (110) with both exhibiting promise as candidate catalysts. Cu or Co ion bound to the HMF oxygen in end-on-structure, HMF molecular is inclined to bridge adsorption. The adsorption energy relies on both the coordination type of surface oxygen to which the hydrogen binds and the possible formation of H-bond involving hydroxy

and formyl groups on the adsorbed HMF. Consistent with DFT calculation, 99% yield of FDCA was obtained with CuO as catalyst under mild conditions (**Table 8**, entry 1). Under same reaction condition, 96% yield of FDCA was attained using Co<sub>3</sub>O<sub>4</sub> as catalyst. Therefore, both CuO and Co<sub>3</sub>O<sub>4</sub> proved as good candidates for the oxidation of HMF-to FDCA.

**Table 8**

HMF oxidation over Cu-based catalyst.

Entry	Catalyst	Oxidant	Base [eq.]	T [°C]	Time [h]	Conv (HMF) [%]	Yield (DFF) [%]	Yield (HMFCA) [%]	Yield (FFCA) [%]	Yield (FDCA) [%]	Ref.
1	CuO	NaClO	NaOH (0.08 eq)	40	2	100	--	--	--	99	[156]
2	CuO	O <sub>2</sub> (9 bar)	Base free	100	15	33	2	3	14	9	[157]
3	CuO-CeO <sub>2</sub>	O <sub>2</sub> (9 bar)	Base free	100	15	99	0	0	90	0	[157]
4	CuCl	TBHP	Base free	RT	48	100	--	--	--	50	[158]
5	SBA-NH <sub>2</sub> (Cu <sup>2+</sup> / VO <sup>2+</sup> )	O <sub>2</sub> (3 bar)	Base free	110	12	99	63	5	--	29	[159]

Another CuO catalyst for HMF oxidation was reported by Ventura et al. [157] using oxygen as an oxidant under base-free conditions, 33% HMF conversion with 14% FFCA yield and 9% FDCA yield was obtained (**Table 8**, entry 2); thus, oxidation was difficult without base despite higher temperature 100 °C or prolonged reaction time of 15 h. CuO-CeO<sub>2</sub> synthesized by high energy milling (HEM) as catalyst under identical condition leads to a quantitative HMF conversion and 90% FFCA yield. Compared to the physical mixture of CuO and CeO<sub>2</sub> in 1:1 molar ratio (which gave 5% HMF conversion and 3% FFCA yield), it implied that CuO-CeO<sub>2</sub> is not just a simple mixture of two oxides. Further characterization indicated the catalytic performance can be ascribed to correct acid/base sites on CuO-CeO<sub>2</sub>. Mannam et al. [160] reported a general protocol using CuCl as catalyst, *tert*-BuOOH as oxidant for the oxidation of primary alcohols to carboxylic acid in MeCN at room temperature [161]. Furthermore, Hansen [158] deployed CuCl and TBHP under mild conditions to obtain 50% FDCA yield under base-free conditions in MeCN (**Table 8**, entry 4). The formation of FDCA-Cu salt in the catalytic system account for the further reaction inhibition. Liu [159] reported SBA-NH<sub>2</sub> immobilized vanadyl (VO<sup>2+</sup>) and cupric Cu<sup>2+</sup> ions for HMF oxidation, 29% FDCA yield could be obtained (**Table 8**, entry 5). The addition of Cu<sup>2+</sup> promoted the generation of active V<sup>5+</sup> species, as the Cu<sup>+</sup> can be easily oxidized into Cu<sup>2+</sup> by oxygen, thus a whole catalytic recycle ensured reaction proceeds; no vanadium and copper leaching could be discerned in recycling experiments indicating that SBA-NH<sub>2</sub> immobilized Cu<sup>2+</sup> and VO<sup>2+</sup> successfully.

#### 2.2.4. Iron (Fe)

Iron as a cheap and earth-abundant element that has been used as a support or an alloy with noble metal for the oxidation of HMF; some representative examples are: Fe, Pd alloy

(**Table 2**, entries 13, 14, 15), a core-shell  $\text{Fe}_3\text{O}_4$  with amorphous carbon as matrix supported Pt (**Table 3**, entry 21),  $\text{Ru}(\text{OH})_2$  (**Table 4**, entry 24) and  $\text{MnFe}_2\text{O}_4$  displayed activation in HMF oxidation (**Table 6**, entries 4, 5). These evidences indicated that Fe is an active element for the oxidation of HMF oxidation as detailed below for Fe-based catalysts.

Fe in-homogeneous form as a catalyst was reported by Fang et al. [162] where  $\text{Fe}(\text{NO}_3)_3 \cdot 9\text{H}_2\text{O}$  system (Fe/TEMPO) in DCE at room temperature in air during 4 h, afforded 92% yield of DFF. The addition of  $\text{Cl}^-$  from NaCl functioned as a special electron-donating ligand to provide electrons to the d orbitals of  $\text{Fe}^{3+}$  to accelerate the coupling with TEMPO. Furthermore, starting from isolated DFF to FDCA, 80% FDCA yield could be attained.

Fe in heterogeneous form as a catalyst Fe/SBA-15 gave poor FDCA yield (4%) with quantitative HMF conversion [163].  $\text{Fe}_3\text{O}_4 @ \text{SiO}_2$  afforded 21% DFF and 10% FFCA selectivity under normal conditions (110 °C, 10 bar  $\text{O}_2$ , 8 h) [164]. Sha et al. [165] reported 79% FDCA formation deploying  $\text{Fe}^{\text{III}}$ -POP-1 as catalyst under mild conditions (base-free, 100 °C, in 10 h, at 10 bar  $\text{O}_2$ ); high surface area and metal active sites on  $\text{Fe}^{\text{III}}$ -POP-1 played an important role in HMF oxidation, the recovered catalyst suggested  $\text{Fe}^{3+}$  oxidation state remained intact after the catalysis. Another base-free, Fe-Co based catalyst nano- $\text{Fe}_3\text{O}_4$ - $\text{CoO}_x$  [166] delivered 68% FDCA under TBHP as an oxidant. Remarkably, the decorated nano- $\text{Fe}_3\text{O}_4$ - $\text{SiO}_2$  with  $-\text{SO}_3\text{H}$  for catalytic conversion of fructose to FDCA *via* two steps, afforded 60% yield of FDCA with no Fe or Co leaching from nano- $\text{Fe}_3\text{O}_4$ - $\text{CoO}_x$ . The economical, and environmentally-friendly advantages of catalyst synthesis and impressive performance-makes it an excellent candidate for scaled-up reaction. Zhang et al. contributed substantially to valorization of biomass-based compounds in ionic liquid (ILs) [167]. A series of Fe-based catalyst ( $\text{Fe}_x\text{Zr}_{0.41-x}\text{O}_2$ ) were synthesized for HMF oxidation,  $\text{Fe}_{0.6}\text{Zr}_{0.4}\text{O}_2$  was found to be the most efficient catalyst in ILs-[Bmin]Cl. The smaller particle size, high specific surface area as well as oxygen vacancy in  $\text{Fe}_{0.6}\text{Zr}_{0.4}\text{O}_2$  benefits to the redox properties and these advantages

no doubt enhanced the catalyst's oxidation strength which could be successively reused for five times.

### 2.2.5. Molybdenum (Mo), Tungsten (W) and Vanadium (V)

Molybdenum (Mo) is a common element that appears in HMF oxidation reactions. For instance, montmorillonite K-10 as a matrix to support molybdenum (VI) complex (K-clay-Mo) was optimized in terms of oxygen, solvent, temperature and base; quantitative HMF conversion with 87% HMFCFA yield was obtained in toluene with flushing of oxygen at 110 °C in 3 h (**Table 9**, entry 1) [167]. Magnetic  $\gamma$ -Fe<sub>2</sub>O<sub>3</sub>@HAP-Mo was optimized as a reusable catalyst in terms of solvent, and temperature, which afforded 96% HMF conversion and 20% FDCA yield as well as 68% DFF yield and 9% HMFCFA yield in 4-chlorotoluene under oxygen flow conditions (**Table 9**, entry 2) [168]. However, the use of aromatic solvents resulted in lower intermediate selectivity which restricted its further applications. Another study compared ammonium octamolybdate and ammonium dactungstate in aq. H<sub>2</sub>O<sub>2</sub> for the oxidation of HMF. The insights into the catalytic performance is depicted where both, quaternary ammonium dactungstate and quaternary ammonium octamolybdate adorn a number of single and double epoxy groups in presence of H<sub>2</sub>O<sub>2</sub>. In both cases, the double epoxy groups functioned as the main active sites for the conversion of HMF to FDCA, but this process was inhibited by steric hindrance for the double epoxy groups attached by a quaternary ammonium in the case of tungsten (W). No steric hindrance occurs in the case of molybdenum (Mo), thus affording 99% FDCA yield with tetra-1-ethyl-3-methylimidazolium octamolybdate ([EMIM]<sub>4</sub>Mo<sub>8</sub>O<sub>26</sub>) as catalyst (**Table 9**, entry 3) [169].

**Table 9**

HMF oxidation over Mo and V-based catalysts.

Entry	Catalyst	Oxidant	Base [eq.]	T [°C]	Time [h]	Conv (HMF) [%]	Yield	Yield	Yield	Ref.
							(DFF) [%]	(HMFCA) [%]	(FDCA) [%]	
1	K-10 clay-Mo	O <sub>2</sub> (20 mL min <sup>-1</sup> )	Base free	110	3	100	--	87	--	[167]
2	γ-Fe <sub>2</sub> O <sub>3</sub> @HAP-Mo	O <sub>2</sub> (20 mL min <sup>-1</sup> )	Base free	120	12	96	68	9	20	[168]
3	[EMIM] <sub>4</sub> Mo <sub>8</sub> O <sub>26</sub>	H <sub>2</sub> O <sub>2</sub> (0.16 mol)	NaOH (2 eq)	100	2	99	0	0	99	[169]
4	VO <sub>x-ms</sub>	O <sub>2</sub> (30 bar)	Base free	130	1	94	89	--	2	[171]
5	V <sub>2</sub> O <sub>5</sub>	O <sub>2</sub> (30 bar)	Base free	130	1	83	77	--	0	[170]
6	VO <sub>2</sub>	O <sub>2</sub> (30 bar)	Base free	130	1	75	66	--	1	[170]
7	V <sub>2</sub> O <sub>3</sub>	O <sub>2</sub> (30 bar)	Base free	130	1	63	57	--	0	[170]

The effect of vanadium-based homogeneous catalysis in HMF oxidation involved a catalytic cycle that involved the reduction of  $V^{5+}$  to  $V^{4+}$  during HMF coupling which was further oxidized  $V^{4+}$  to  $V^{5+}$  by  $O_2$  [171] in  $VO_x/TiO_2$  system [172]. Vanadium phosphate oxide (VPO) based heterogeneous catalysts,  $C_{14}VOPO_4$  and  $C_{14}VOHPO_4$  delivered 83% DFF yield in toluene using  $O_2$  at 110 °C [173]. Furthermore, Yan et al. synthesized nanobelt-arrayed vanadium hierarchical microspheres ( $VO_x$ -ms) which gave 93% HMF conversion and 89% DFF yield, an advantage when compared to the commercial  $V_2O_5$ ,  $VO_2$  and  $V_2O_3$  under identical optimum conditions for HMF conversion and DFF yield (**Table 9**, entry 4 vs 5-7) [170]. Mechanistically, HMF adsorbed preferably on the catalyst surface  $V=O$  sites on facet (010) due to the strong hydrogen adsorption capability (Step 1). Subsequently, the intermediate  $RCH_2OVOH$  is irreversibly oxidized to form DFF by lattice oxygen of  $V=O$  (Step 2). Finally, the third step was the regeneration of  $V=O$  by oxygen.

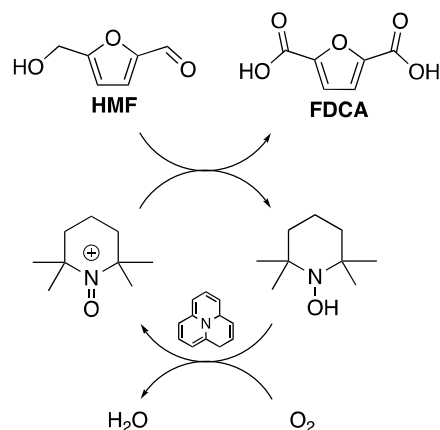
Bimetallics incorporating Mo and V have been widely reported in heteropolyacid or polyoxometalate based catalysts [174]. The synergetic effect between Mo, V and other elements as well as the unique physical mesoporous, morphology, multifunctional sites of redox, acidic/basic support property were attributed to HMF oxidation. However, most of them showed low catalytic activity towards FDCA, although—intermediates like DFF, HMFCAs were broadly reported. For instance, polyoxometalate  $H_5PMo_{10}V_2O_{40}/SiO_2$  (HPMoV/SiO<sub>2</sub>) gave 89% DFF yield in presence of oxygen at 120 °C during 8 h [175]. Furthermore, Li et al. reported that HPMoV@surf(n)/CeO<sub>2</sub> delivered 95.3% DFF yield with complete HMF conversion in DMSO as a solvent under 10 bar  $O_2$ , at 120 °C in 6 h [176].

### 2.3. Metal free catalysts

Metal-free conditions, from the economic and green chemistry point of view has garnered more attentions as a sustainable alternative to metal-based catalysts.

### 2.3.1. Carbonaceous material

Nitrogen-doped carbon materials (NCs) were among the first ones reported for HMF oxidation. For instance, Nguyen et al. obtained nanoporous nitrogen-doped carbon (NNC) *via* the pyrolysis of zeolitic-imidazole framework (ZIF-8). And the ensuing graphitic nitrogen (N-Q) structure in NNC-900 contributed to FDCA formation, 80% FDCA yield under optimum conditions (3 eq.  $K_2CO_3$ , 100 ml/min oxygen flow, 80 °C during 48 h) [177]. Another investigation reported N-doped AC as catalyst that could afford 24% HMF conversion with 93% DFF selectivity under mild condition (80 °C, 15 h) [178]. Furthermore, nitrogen-doped graphene material with 2,2,6,6-tetramethylpiperidin-oxyl (TEMPO) as co-catalyst has been examined for HMF oxidation to DFF [179]. The synergistic effect between TEMPO and nitrogen species doped on graphene lattice as well as molecular oxygen contributed to 100% HMF conversion, 99.5% DFF yield under optimum conditions (NG-900 in acetonitrile, TEMPO 1 mmol, 1 bar  $O_2$  in 100 °C, 3 h); proposed catalytic cycle-being depicted in **Scheme 6**. Molecular oxygen initially adsorbed on the graphitic type nitrogen atom, TEMPO was oxidized to oxoammonium cation, HMF was oxidized to DFF at the same time, with the formation of hydroxylamine. Sequentially, the hydroxylamine derivative was re-oxidized by oxygen molecular to generate TEMPO to realize a new catalytic cycle. The N species involved in graphitic active sites play an important role in adsorbing and activating the oxygen.



**Scheme 6.** Possible reaction pathway for oxidation of HMF in NG-TEMPO catalytic system.

J. Zhao et al. [180] reported a variety of substituted anthraquinones for the catalytic oxidation of alcohol to the corresponding carbonyl compounds; 42% DFF and 56% FDCA yields were obtained using 2,6-dihydroxyanthraquinone (DAQ) as catalyst under optimum conditions (toluene as solvent, 10 bar O<sub>2</sub>, at 130°C, in 2 h).

Another carbonaceous material, porous chitosan-derived material (PCNx) (*via* calcination of chitosan at 300 °C in nitrogen atmosphere for 4 h) served as a catalyst for the oxidation of HMF to FDCA was reported by Verma et al. [181], 83% FDCA was obtained under optimum conditions (1 eq. K<sub>2</sub>CO<sub>3</sub>, 70°C, 36 h). The graphitic nitrogen in PCNx plays an important role in oxygen activation. The impressive FDCA yield and good recyclability, up to five successive runs, paved the way towards the rational design of marine-based nano-catalysts for special catalytic transformations.

### 2.3.2. Biocatalysts

Biotransformation is eco-friendly process that often involves mild reaction condition, less toxic chemicals requirement or regeneration. However, biocatalyst for HMF oxidation showed less efficiency when compared to metal-based catalysts as they required longer reaction times, final oxidation product-FDCA was rarely formed, importantly, catalyst

recyclability is hard. Therefore, the bioactive HMF oxidation still remains a big challenge for research community.

Biocatalysis involves whole-cells and enzymes as two main processes. For instance, whole-cell biocatalyst *Deinococcus wulumuqiensis* R12 used in HMF oxidation to HMFCFA reported by Cang et al. [182]; 90% HMFCFA was obtained when HMF concentration was 300 mM during 36 h, a higher productivity of 44 g L<sup>-1</sup> per day by employing a fed-batch process. Remarkably, the cells were able to transform a variety of aldehyde compounds into corresponding carboxylic acid. Another impressive whole-cells biocatalyst *Gluconobacteroxydans* DSM 50049 gave 94% HMFCFA yield within 17 h [183] where high purity of recovered HMFCFA was achieved by anion exchange resins (Amberlite IRA-400). Furthermore, *Cupriavidus basilensis* HMF 14 resulted in 30.1 g L<sup>-1</sup> FDCA productivity at a yield of FDCA 97% in fed-batch experiment [184].

Likewise, enzymatic methods, for instance, lipases and oxidases have been widely reported for the oxidation of HMF-[185]. Krystof et al. [186] reported a commercial lipases B from *Candida Antarctica* for oxidation of HMF to DFF which was then converted to FDCA in 93%-yield deploying lipases as biocatalyst and alkyl esters as acyl donors upon addition of H<sub>2</sub>O<sub>2</sub> (30% v/v). Carro et al. [187] investigated fungal aryl-alcohol oxidase (AAO), which was unable to oxidize FFCA into FDCA; 98% yield of FFCA was obtained using AAO as catalyst with the generation of H<sub>2</sub>O<sub>2</sub>. Further addition of another oxidase (*A. aegerita*, UPO) assisted the conversion of FFCA to FDCA in 91% yield, in 120 h. Lately, Serrano et al. found that in AAO biocatalytic system, the produced H<sub>2</sub>O<sub>2</sub> in the first step has an inhibitory effect for next oxidation step. The use of catalase to remove H<sub>2</sub>O<sub>2</sub> from the system leads to 99% conversion of HMF to FDCA without addition of another biocatalyst [188]. Mckenna et al. [189] reported a continuous oxidation of HMF to FDCA using galactose oxidase M<sub>3-5</sub> variant (GOaseM<sub>3-5</sub>), periplasmic aldehyde oxidase (PaoABC) and horse radish peroxidase (HRP), the synergetic

effect between three oxidases afforded 100% FDCA yield under optimum conditions (100 mM HMF, 0.2 mM Kpi PH=7, 37 °C, 3 h). A cloning of gene from *Methylovorus sp. Strain MP688* encode HMFO (a member of glucose-methanol-choline (GMC-type) oxidase family), delivered 92% FFCA and 8% FDCA obtained with HMFO as a catalyst [190]. Remarkably, the same group reported HMFO as biocatalyst to secure 95% FDCA yield under another optimum condition (25 °C, potassium phosphate buffer pH=7, 24 h) [191] with four consecutive oxidation steps by recycling of HMFO.

### 3. Conclusions and perspectives

The oxidation of HMF to produce FDCA and other high value intermediates was illustrated in highly efficient pathways. The tremendous value of these compounds not only play an important role in biomass-based products to generate financial reward advantages, but also reduce the reliance on fossil-derived resources, to achieve the goal of green chemistry and environmental protection. Catalytic system for the oxidation of HMF in conventional batch condition has been investigated, comprehensively. Heterogeneous catalytic systems show easy separation and good catalyst recycling advantages than homogeneous catalyst, and hence being widely investigated. With different noble metals, HMF oxidation routes are different. For instance, the oxidation of aldehydic side chain of HMF to carboxylic group was more efficient over Au-based catalyst, while Pd, and Pt oxidize and activate the alcoholic portion of HMFCFA to FDCA effectively under basic condition. However, mono-noble metals have limitations of higher cost, and poor recyclability. Non-noble catalysts are good alternatives but they have the drawbacks of low HMF/metal molar ratio, and low FDCA yield and selectivity. The bimetallic alloy catalysts display improved catalytic performance as well as catalytic recyclability. The use of oxygen as oxidant possess salient advantages than other oxidants. Noticeably, isotope labeling analysis showed that the oxygen is incorporated from

water to FDCA rather than oxygen. From the mechanistic viewpoint, oxygen scavenged the electrons to close the catalytic cycle, and suppress the side reactions thus realizing the durability aspects of the catalyst but high oxygen pressure is required which is the reason water has been used as a common solvent for HMF oxidation. Homogeneous catalysts can accelerate nucleophilic attack of aldehyde group to carboxylic group, thus accelerating the reaction rate. Heterogeneous ~~base~~ catalysts show the alternative pathway from the perspective of economic and green chemistry although they still suffered from leaching and low selectivity for FDCA. Catalyst support, particle size, the active sites distribution on the support dramatically influenced the results as well as temperature, oxidant pressure and HMF concentration. Biocatalysts displayed quantitative HMF conversion and FDCA yield under mild conditions, however, the low HMF substrate concentration and the catalyst productivity have been a barrier for their application.

Despite all the efforts expanded on the oxidation of HMF in the laboratory settings, these are some drawbacks that hinder the industrial production of FDCA *via* the oxidation of HMF from derived high value intermediates. From the point view of keeping a balance between green chemistry and commercial economics, three major challenges need to be addressed in future: i) high cost of processing, ii) defects in catalytic systems, and iii) complete assessment of the intensification processes.

FDCA production process rely more on the oxidation of HMF. In some cases, HMF has an equal or even higher price than FDCA. The starting material, HMF itself, deserves more attention for industrialization production. The complete utilization of other lignocellulosic biomass resources like cellulose, glucose and fructose as starting material for FDCA or other value oxidation intermediates secured in one-pot operation deserves more exploration. In that case, cheaper starting materials, avoiding the for separation of need HMF will no doubt improve the economic feasibility.

Bimetallic catalysts or alloying with other metals as catalyst showed promising results with improved catalytic ability and stability when compared to mono noble metal. Non-noble metals certainly deserve exploratory attentions. Additionally, multi-functional catalysts need rational design for use in lignocellulosic resources as starting material to target compounds in one-pot operation.

Large-scale production of chemicals needs to be emphasized in relation to laboratory-scale curiosity-driven catalytic reaction. Many current methods are technically feasible, but not economical. We believe that further progress will be realized in future biorefineries by particularly exploiting multidisciplinary approach and multi-functional heterogeneous catalysts to ensure the highly coveted and desirable sustainable development.

## **Acknowledgements**

Deyang Zhao would like to thank the China Scholarship Council (CSC) for the financial support.

## **References**

- [1] H. Kobayashi, A. Fukuoka, Synthesis and utilisation of sugar compounds derived from lignocellulosic biomass, *Green Chem.* 15 (2013) 1740-1763, <https://doi.org/10.1039/c3gc00060e>.
- [2] S. Morales-delaRosa, J.M. Campos-Martin, J.L.G. Fierro, Optimization of the process of chemical hydrolysis of cellulose to glucose, *Cellulose* 21 (2014) 2397–2407, <https://doi.org/10.1007/s10570-014-0280-9>.
- [3] F. Delbecq, C. Len, Recent advances in the microwave-assisted production of hydroxymethylfurfural by hydrolysis of cellulose derivatives - A review, *Molecules* 23 (2018) 1973, <https://doi.org/10.3390/molecules23081973>.

- [4] T.W. Tzeng, P. Bhaumik, P.W. Chung, Understanding the production of 5-hydroxymethylfurfural (HMF) from chitosan using solid acids, *Mol. Catal.* 479 (2019) 110627, <https://doi.org/10.1016/j.mcat.2019.110627>.
- [5] S.F. Mayer, H. Falcon, R. Dipaola, P. Ribota, L. Moyano, S. Morales-delaRosa, R. Mariscal, J.M. Campos-Martin, J.A. Alonso, J.L.G. Fierro, Dehydration of fructose to HMF in presence of  $(\text{H}_3\text{O})_x\text{Sb}_x\text{Te}_{(2-x)}\text{O}_6$  ( $x=1, 1.1, 1.25$ ) in  $\text{H}_2\text{O}$ -MIBK, *Mol. Catal.* 481 (2020) 110276, <https://doi.org/10.1016/j.mcat.2018.12.025>.
- [6] J. Tacacima, S. Derenzo, J.G. Rocha Poco, Synthesis of HMF from fructose using Purolite® strong acid catalyst: comparison between BTR and PBR reactor type for kinetics data acquisition, *Mol. Catal.* 458 (2018) 180-188, <https://doi.org/10.1016/j.mcat.2017.12.021>.
- [7] C. Xu, E. Paone, D. Rodriguez-Padron, R. Luque, F. Mauriello, Recent catalytic routes for the preparation and the upgrading of biomass derived furfural and 5-hydroxymethylfurfural, *Chem. Soc. Rev.* 49 (2020) 4273-4306, <https://doi.org/10.1039/D0CS00041H>.
- [8] K. Gupta, R.K. Rai, S.K. Singh, Metal catalysts for the efficient transformation of biomass derived HMF and furfural to value added chemicals, *ChemCatChem* 10 (2018) 2326-2349, <https://doi.org/10.1002/cctc.201701754>.
- [9] H. Xia, S. Xu, H. Hu, J. An, C. Li, Efficient conversion of 5-hydroxymethylfurfural to high-value chemicals by chemo- and bio-catalysis, *RSC Adv.* 8 (2018) 30875-30886, <https://doi.org/10.1039/C8RA05308A>.
- [10] Z. Zhang, G.W. Huber, Catalytic oxidation of carbohydrates into organic acids and furan chemicals, *Chem. Soc. Rev.* 47 (2018) 1351-1390, <https://doi.org/10.1039/C7CS00213K>.
- [11] P.L. Arias, J.A. Cecilia, I. Gandarias, J. Iglesias, M. López Granados, R. Mariscal, G.

- Morales, R. Moreno-Tost, P. Maireles-Torres, Oxidation of lignocellulosic platform molecules to value-added chemicals using heterogeneous catalytic technologies, *Catal. Sci. Technol.* 10 (2020) 2721–2757, <https://doi.org/10.1039/D0CY00240B>.
- [12] Y. Liao, B.O. de Beeck, K. Thielemans, T. Ennaert, J. Snelders, M. Dusselier, C.M. Courtin, B.F. Sels, The role of pretreatment in the catalytic valorization of cellulose, *Mol. Catal.* 487 (2020) 110883, <https://doi.org/10.1016/j.mcat.2020.110883>
- [13] B. Liu, Z. Zhang, One-Pot Conversion of carbohydrates into furan derivatives via furfural and 5-hydroxymethylfurfural as intermediates, *ChemSusChem* 9 (2016) 2015–2036, <https://doi.org/10.1002/cssc.201600507>.
- [14] Q. Lei, J. Li, N. Cao, Z. Song, C.L. Liu, W.S. Dong, Direct production of 2,5-diformylfuran from fructose catalysed by Mo-based composite oxides in static air, *Mol. Catal.* 487 (2020) 110892, <https://doi.org/10.1016/j.mcat.2020.110892>
- [15] A.C. Braisted, J.D. Oslob, W.L. Delano, J. Hyde, R.S. McDowell, N. Waal, C. Yu, M.R. Arkin, B.C. Raimundo, Discovery of a potent small molecule IL-2 inhibitor through fragment assembly, *J. Am. Chem. Soc.* 125 (2003) 3714–3715, <https://doi.org/10.1021/ja034247i>.
- [16] M. Munekata, G. Tamura, Antitumor activity of 5-hydroxymethyl-2-furoic acid, *Agric. Biol. Chem.* 45 (1981) 2149–2150, <https://doi.org/10.1080/00021369.1981.10864851>.
- [17] A.F. Sousa, C. Vilela, A.C. Fonseca, M. Matos, C.S.R. Freire, G.-J.M. Gruter, J.F.J. Coelho, A.J.D. Silvestre, Biobased polyesters and other polymers from 2,5-furandicarboxylic acid: a tribute to furan excellency, *Polym. Chem.* 6 (2015) 5961–5983, <https://doi.org/10.1039/C5PY00686D>.
- [18] T. Werpy, G. Petersen, Top value added chemicals from biomass: Volume I - Results of screening for potential candidates from sugars and synthesis gas, 2004,

<https://doi.org/10.2172/15008859>.

- [19] X. Tong, S. Xue, J. Hu, Catalytic production of 5-hydroxymethylfurfural from biomass and biomass-derived sugars, in: Z. Fang, R.L. Smith, X. Qi (Eds.), *Production of platform chemicals from sustainable resources*, Springer Singapore, Singapore, 2017: pp. 81–121, [https://doi.org/10.1007/978-981-10-4172-3\\_3](https://doi.org/10.1007/978-981-10-4172-3_3).
- [20] J.C. Lewis, Germination of bacterial spores by calcium chelates of dipicolinic acid analogues, *J. Biol. Chem.* 1972, 274, 1861-1868.
- [21] M. Duennenberger, M. Schellenbaum, Swiss Patent, CH 532890, 1973; *Chem. Abstr.* 1973, 78, p159405t., n.d.
- [22] J. Lewkowski, Synthesis, chemistry and applications of 5-hydroxymethylfurfural and its derivatives, *Arkivoc* 1 (2001), 17-54, <https://doi.org/10.3998/ark.5550190.0002.102>.
- [23] W. Fraefel, H.F. Lichti, M. Brunetti, US Patent, 4383832, 1983.
- [24] A.J.J.E. Eerhart, A.P.C. Faaij, M.K. Patel, Replacing fossil based PET with biobased PEF; process analysis, energy and GHG balance, *Energy Environ. Sci.* 5 (2012) 6407-6422, <https://doi.org/10.1039/c2ee02480b>.
- [25] G. Chen, N.M. van Straalen, D. Roelofs, The ecotoxicogenomic assessment of soil toxicity associated with the production chain of 2,5-furandicarboxylic acid (FDCA), a candidate bio-based green chemical building block, *Green Chem.* 18 (2016) 4420–4431, <https://doi.org/10.1039/C6GC00430J>.
- [26] Y.Y. Gorbanev, S.K. Klitgaard, J.M. Woodley, C.H. Christensen, A. Riisager, Gold-catalyzed aerobic oxidation of 5-hydroxymethylfurfural in water at ambient temperature, *ChemSusChem* 2 (2009) 672–675, <https://doi.org/10.1002/cssc.200900059>.
- [27] S.E. Davis, B.N. Zope, R.J. Davis, On the mechanism of selective oxidation of 5-

- hydroxymethylfurfural to 2,5-furandicarboxylic acid over supported Pt and Au catalysts, *Green Chem.* 14 (2012) 143–147, <https://doi.org/10.1039/C1GC16074E>.
- [28] A.A. Rosatella, S.P. Simeonov, R.F.M. Frade, C.A.M. Afonso, 5-Hydroxymethylfurfural (HMF) as a building block platform: Biological properties, synthesis and synthetic applications, *Green Chem.* 13 (2011) 754–793, <https://doi.org/10.1039/c0gc00401d>.
- [29] J. Cai, H. Ma, J. Zhang, Q. Song, Z. Du, Y. Huang, J. Xu, Gold nanoclusters confined in a supercage of Y zeolite for aerobic oxidation of HMF under mild conditions, *Chem. Eur. J.* 19 (2013) 14215–14223, <https://doi.org/10.1002/chem.201301735>.
- [30] Q. Li, H. Wang, Z. Tian, Y. Weng, C. Wang, J. Ma, C. Zhu, W. Li, Q. Liu, L. Ma, Selective oxidation of 5-hydroxymethylfurfural to 2,5-furandicarboxylic acid over Au/CeO<sub>2</sub> catalysts: the morphology effect of CeO<sub>2</sub>, *Catal. Sci. Technol.* 9 (2019) 1570–1580, <https://doi.org/10.1039/C9CY00211A>.
- [31] S. Albonetti, A. Lolli, V. Morandi, A. Migliori, C. Lucarelli, F. Cavani, Conversion of 5-hydroxymethylfurfural to 2,5-furandicarboxylic acid over Au-based catalysts: Optimization of active phase and metal–support interaction, *Appl. Catal. B: Environmental* 163 (2015) 520–530, <https://doi.org/10.1016/j.apcatb.2014.08.026>.
- [32] M. Ventura, F. Nocito, E. de Giglio, S. Cometa, A. Altomare, A. Dibenedetto, Tunable mixed oxides based on CeO<sub>2</sub> for the selective aerobic oxidation of 5-(hydroxymethyl)furfural to FDCA in water, *Green Chem.* 20 (2018) 3921–3926, <https://doi.org/10.1039/C8GC00972D>.
- [33] D. Yan, J. Xin, C. Shi, X. Lu, L. Ni, G. Wang, S. Zhang, Base-free conversion of 5-hydroxymethylfurfural to 2,5-furandicarboxylic acid in ionic liquids, *Chem. Eng. J.* 323 (2017) 473–482, <https://doi.org/10.1016/j.cej.2017.04.021>.

- [34] M. Ventura, F. Lobefaro, E. de Giglio, M. Distaso, F. Nocito, A. Dibenedetto, Selective aerobic oxidation of 5-hydroxymethylfurfural to 2,5-diformylfuran or 2-formyl-5-furancarboxylic Acid in water by using MgOCeO<sub>2</sub> mixed oxides as catalysts, *ChemSusChem*. 11 (2018) 1305–1315. <https://doi.org/10.1002/cssc.201800334>.
- [35] F. Nocito, M. Ventura, M. Aresta, A. Dibenedetto, Selective oxidation of 5-(hydroxymethyl)furfural to DFF using water as solvent and oxygen as oxidant with earth-crust-abundant mixed oxides, *ACS Omega* 3 (2018) 18724–18729, <https://doi.org/10.1021/acsomega.8b02839>.
- [36] C. Megías-Sayago, K. Chakarova, A. Penkova, A. Lolli, S. Ivanova, S. Albonetti, F. Cavani, J.A. Odriozola, Understanding the role of the acid sites in HMF oxidation to FDCA reaction over gold catalysts: surface investigation on CexZr1-xO<sub>2</sub> compounds, *ACS Catal.* 8 (2018) 11154–11164, <https://doi.org/10.1021/acscatal.8b02522>
- [37] G.J. Hutchings, Nanocrystalline gold catalysts: A reflection on catalyst discovery and the nature of active sites, *Gold Bull.* 42 (2009) 260–266, <https://doi.org/10.1007/BF03214947>.
- [38] Y. Kuwauchi, H. Yoshida, T. Akita, M. Haruta, S. Takeda, Intrinsic catalytic structure of gold nanoparticles supported on TiO<sub>2</sub>, *Angew. Chem.* 124 (2012) 7849–7853, <https://doi.org/10.1002/ange.201201283>.
- [39] W. Song, E.J.M. Hensen, A computational DFT study of CO oxidation on a Au nanorod supported on CeO<sub>2</sub>(110): on the role of the support termination, *Catal. Sci. Technol.* 3 (2013) 3020–3029, <https://doi.org/10.1039/c3cy00319a>.
- [40] M. Wang, F. Wang, J. Ma, M. Li, Z. Zhang, Y. Wang, X. Zhang, J. Xu, Investigations on the crystal plane effect of ceria on gold catalysis in the oxidative

- dehydrogenation of alcohols and amines in the liquid phase, *Chem. Commun.* 50 (2014) 292–294, <https://doi.org/10.1039/C3CC46180G>.
- [41] O. Casanova, S. Iborra, A. Corma, Biomass into chemicals: Aerobic oxidation of 5-hydroxymethyl-2-furfural into 2,5-furandicarboxylic acid with gold nanoparticle catalysts, *ChemSusChem* 2 (2009) 1138–1144, <https://doi.org/10.1002/cssc.200900137>.
- [42] M. Kim, Y. Su, A. Fukuoka, E.J.M. Hensen, K. Nakajima, Aerobic oxidation of 5-(hydroxymethyl)furfural cyclic acetal enables selective furan-2,5-dicarboxylic acid formation with CeO<sub>2</sub>-Supported Gold Catalyst, *Angew. Chem. Int. Ed.* 57 (2018) 8235–8239, <https://doi.org/10.1002/anie.201805457>.
- [43] Z. Miao, Y. Zhang, X. Pan, T. Wu, B. Zhang, J. Li, T. Yi, Z. Zhang, X. Yang, Superior catalytic performance of Ce<sub>1-x</sub>Bi<sub>x</sub>O<sub>2-δ</sub> solid solution and Au/Ce<sub>1-x</sub>Bi<sub>x</sub>O<sub>2-δ</sub> for 5-hydroxymethylfurfural conversion in alkaline aqueous solution, *Catal. Sci. Technol.* 5 (2015) 1314–1322, <https://doi.org/10.1039/C4CY01060D>.
- [44] T. Pasini, M. Piccinini, M. Blosi, R. Bonelli, S. Albonetti, N. Dimitratos, J.A. Lopez-Sanchez, M. Sankar, Q. He, C.J. Kiely, G.J. Hutchings, F. Cavani, Selective oxidation of 5-hydroxymethyl-2-furfural using supported gold–copper nanoparticles, *Green Chem.* 13 (2011) 2091–2099. <https://doi.org/10.1039/c1gc15355b>.
- [45] C.A. Antonyraj, N.T.T. Huynh, S.-K. Park, S. Shin, Y.J. Kim, S. Kim, K.-Y. Lee, J.K. Cho, Basic anion-exchange resin (AER)-supported Au-Pd alloy nanoparticles for the oxidation of 5-hydroxymethyl-2-furfural (HMF) into 2,5-furan dicarboxylic acid (FDCA), *Appl. Catal. A: General* 547 (2017) 230–236, <https://doi.org/10.1016/j.apcata.2017.09.012>.
- [46] Q. Wang, W. Hou, S. Li, J. Xie, J. Li, Y. Zhou, J. Wang, Hydrophilic mesoporous poly(ionic liquid)-supported Au–Pd alloy nanoparticles towards aerobic oxidation of

- 5-hydroxymethylfurfural to 2,5-furandicarboxylic acid under mild conditions, *Green Chem.* 19 (2017) 3820–3830, <https://doi.org/10.1039/C7GC01116D>.
- [47] Z. Gui, W. Cao, S. Saravanamurugan, A. Riisager, L. Chen, Z. Qi, Efficient aerobic oxidation of 5-hydroxymethylfurfural in aqueous media with Au-Pd supported on zinc hydroxycarbonate, *ChemCatChem* 8 (2016) 3636–3643, <https://doi.org/10.1002/cctc.201600852>.
- [48] A. Villa, M. Schiavoni, S. Campisi, G.M. Veith, L. Prati, Pd-modified Au on carbon as an effective and durable catalyst for the direct oxidation of HMF to 2,5-furandicarboxylic acid, *ChemSusChem* 6 (2013) 609–612, <https://doi.org/10.1002/cssc.201200778>.
- [49] D. Bonincontro, A. Lolli, A. Villa, L. Prati, N. Dimitratos, G.M. Veith, L.E. Chinchilla, G.A. Botton, F. Cavani, S. Albonetti, AuPd-nNiO as an effective catalyst for the base-free oxidation of HMF under mild reaction conditions, *Green Chem.* 21 (2019) 4090–4099, <https://doi.org/10.1039/C9GC01283D>.
- [50] Z. Gao, R. Xie, G. Fan, L. Yang, F. Li, Highly efficient and stable bimetallic AuPd over La-doped Ca–Mg–Al layered double hydroxide for base-free aerobic oxidation of 5-hydroxymethylfurfural in water, *ACS Sustainable Chem. Eng.* 5 (2017) 5852–5861, <https://doi.org/10.1021/acssuschemeng.7b00573>.
- [51] X. Wan, C. Zhou, J. Chen, W. Deng, Q. Zhang, Y. Yang, Y. Wang, Base-free aerobic oxidation of 5-hydroxymethylfurfural to 2,5-furandicarboxylic acid in water catalyzed by functionalized carbon nanotube-supported Au–Pd alloy nanoparticles, *ACS Catal.* 4 (2014) 2175–2185, <https://doi.org/10.1021/cs5003096>.
- [52] C.P. Ferraz, M. Zieliński, M. Pietrowski, S. Heyte, F. Dumeignil, L.M. Rossi, R. Wojcieszak, Influence of support basic sites in green oxidation of biobased substrates using Au-promoted catalysts, *ACS Sustainable Chem. Eng.* 6 (2018) 16332–16340,

<https://doi.org/10.1021/acssuschemeng.8b03330>.

- [53] N.K. Gupta, S. Nishimura, A. Takagaki, K. Ebitani, Hydrotalcite-supported gold-nanoparticle-catalyzed highly efficient base-free aqueous oxidation of 5-hydroxymethylfurfural into 2,5-furandicarboxylic acid under atmospheric oxygen pressure, *Green Chem.* 13 (2011) 824-827, <https://doi.org/10.1039/c0gc00911c>.
- [54] T. Gao, T. Gao, W. Fang, Q. Cao, Base-free aerobic oxidation of 5-hydroxymethylfurfural to 2,5-furandicarboxylic acid in water by hydrotalcite-activated carbon composite supported gold catalyst, *Mol. Catal.* 439 (2017) 171–179, <https://doi.org/10.1016/j.mcat.2017.06.034>.
- [55] O.R. Schade, K.F. Kalz, D. Neukum, W. Kleist, J.-D. Grunwaldt, Supported gold- and silver-based catalysts for the selective aerobic oxidation of 5-(hydroxymethyl)furfural to 2,5-furandicarboxylic acid and 5-hydroxymethyl-2-furancarboxylic acid, *Green Chem.* 20 (2018) 3530–3541, <https://doi.org/10.1039/C8GC01340C>.
- [56] N. Masoud, B. Donoeva, P.E. de Jongh, Stability of gold nanocatalysts supported on mesoporous silica for the oxidation of 5-hydroxymethyl furfural to furan-2,5-dicarboxylic acid, *Appl. Catal. A: General* 561 (2018) 150–157, <https://doi.org/10.1016/j.apcata.2018.05.027>.
- [57] C. Megías-Sayago, A. Lolli, S. Ivanova, S. Albonetti, F. Cavani, J.A. Odriozola, Au/Al<sub>2</sub>O<sub>3</sub> – Efficient catalyst for 5-hydroxymethylfurfural oxidation to 2,5-furandicarboxylic acid, *Catal. Today* 333 (2019) 169–175, <https://doi.org/10.1016/j.cattod.2018.04.024>.
- [58] B. Saha, S. Dutta, M.M. Abu-Omar, Aerobic oxidation of 5-hydroxymethylfurfural with homogeneous and nanoparticulate catalysts, *Catal. Sci. Technol.* 2 (2012) 79–81, <https://doi.org/10.1039/C1CY00321F>.

- [59] B.N. Zope, S.E. Davis, R.J. Davis, Influence of Reaction Conditions on diacid formation during Au-catalyzed oxidation of glycerol and hydroxymethylfurfural, *Top Catal.* 55 (2012) 24–32, <https://doi.org/10.1007/s11244-012-9777-3>.
- [60] J.M.R. Gallo, D.M. Alonso, M.A. Mellmer, J.A. Dumesic, Production and upgrading of 5-hydroxymethylfurfural using heterogeneous catalysts and biomass-derived solvents, *Green Chem.* 15 (2013) 85–90, <https://doi.org/10.1039/C2GC36536G>.
- [61] B. Donoeva, N. Masoud, P.E. de Jongh, Carbon support surface effects in the gold-catalyzed oxidation of 5-hydroxymethylfurfural, *ACS Catal.* 7 (2017) 4581–4591, <https://doi.org/10.1021/acscatal.7b00829>.
- [62] L. Ardemani, G. Cibin, A.J. Dent, M.A. Isaacs, G. Kyriakou, A.F. Lee, C.M.A. Parlett, S.A. Parry, K. Wilson, Solid base catalysed 5-HMF oxidation to 2,5-FDCA over Au/hydrotalcites: fact or fiction?, *Chem. Sci.* 6 (2015) 4940–4945, <https://doi.org/10.1039/C5SC00854A>.
- [63] K. Kaneda, T. Mitsudome, Coinage metal nanoparticles on hydrotalcite - Gold nanoparticles on hydrotalcite, in: John Wiley & Sons, Ltd (Ed.), *Encyclopedia of Reagents for Organic Synthesis*, John Wiley & Sons, Ltd, Chichester, UK, 2013: p. rn01607. <https://doi.org/10.1002/047084289X.rn01607>.
- [64] G. Yi, S.P. Teong, X. Li, Y. Zhang, Purification of biomass-derived 5-hydroxymethylfurfural and its catalytic conversion to 2,5-furandicarboxylic acid, *ChemSusChem* 7 (2014) 2131–2135, <https://doi.org/10.1002/cssc.201402105>.
- [65] H. Xia, J. An, M. Hong, S. Xu, L. Zhang, S. Zuo, Aerobic oxidation of 5-hydroxymethylfurfural to 2,5-difurancarboxylic acid over Pd-Au nanoparticles supported on Mg-Al hydrotalcite, *Catal. Today* 319 (2019) 113–120, <https://doi.org/10.1016/j.cattod.2018.05.050>.
- [66] A. Lolli, S. Albonetti, L. Utili, R. Amadori, F. Ospitali, C. Lucarelli, F. Cavani,

Insights into the reaction mechanism for 5-hydroxymethylfurfural oxidation to FDCA on bimetallic Pd–Au nanoparticles, *Appl. Catal. A: General* 504 (2015) 408–419, <https://doi.org/10.1016/j.apcata.2014.11.020>.

- [67] S.E. Davis, L.R. Houk, E.C. Tamargo, A.K. Datye, R.J. Davis, Oxidation of 5-hydroxymethylfurfural over supported Pt, Pd and Au catalysts, *Catal. Today* 160 (2011) 55–60, <https://doi.org/10.1016/j.cattod.2010.06.004>.
- [68] P.V. Rathod, V.H. Jadhav, Efficient method for synthesis of FDCA from 5-hydroxymethylfurfural and fructose using Pd/CC catalyst under aqueous conditions, *ACS Sustainable Chem. Eng.* 6 (2018) 5766–5771, <https://doi.org/10.1021/acssuschemeng.7b03124>.
- [69] J.C. Espinosa, R.C. Contreras, S. Navalón, C. Rivera-Cárcamo, M. Álvaro, B.F. Machado, P. Serp, H. Garcia, Influence of carbon supports on palladium nanoparticle activity toward hydrodeoxygenation and aerobic oxidation in biomass transformations: Influence of carbon supports on palladium nanoparticle activity toward hydrodeoxygenation and aerobic oxidation in biomass transformations, *Eur. J. Inorg. Chem.* 2019 (2019) 1979–1987, <https://doi.org/10.1002/ejic.201900190>.
- [70] M.S. Ahmed, D.S. Mannel, T.W. Root, S.S. Stahl, Aerobic oxidation of diverse primary alcohols to carboxylic acids with a heterogeneous Pd–Bi–Te/C (PBT/C) catalyst, *Org. Process Res. Dev.* 21 (2017) 1388–1393, <https://doi.org/10.1021/acs.oprd.7b00223>.
- [71] C. Chen, X. Li, L. Wang, T. Liang, L. Wang, Y. Zhang, J. Zhang, Highly porous nitrogen- and phosphorus-codoped graphene: An outstanding support for Pd catalysts to oxidize 5-hydroxymethylfurfural into 2,5-furandicarboxylic acid, *ACS Sustainable Chem. Eng.* 5 (2017) 11300–11306, <https://doi.org/10.1021/acssuschemeng.7b02049>.

- [72] B. Siyo, M. Schneider, M.-M. Pohl, P. Langer, N. Steinfeldt, Synthesis, characterization, and application of PVP-Pd NP in the aerobic oxidation of 5-hydroxymethylfurfural (HMF), *Catal. Lett.* 144 (2014) 498–506, <https://doi.org/10.1007/s10562-013-1186-0>.
- [73] D. Lei, K. Yu, M.-R. Li, Y. Wang, Q. Wang, T. Liu, P. Liu, L.-L. Lou, G. Wang, S. Liu, Facet effect of single-crystalline Pd nanocrystals for aerobic oxidation of 5-hydroxymethyl-2-furfural, *ACS Catal.* 7 (2017) 421–432, <https://doi.org/10.1021/acscatal.6b02839>.
- [74] B. Siyo, M. Schneider, J. Radnik, M.-M. Pohl, P. Langer, N. Steinfeldt, Influence of support on the aerobic oxidation of HMF into FDCA over preformed Pd nanoparticle based materials, *Appl. Catal. A: General* 478 (2014) 107–116, <https://doi.org/10.1016/j.apcata.2014.03.020>.
- [75] N. Mei, B. Liu, J. Zheng, K. Lv, D. Tang, Z. Zhang, A novel magnetic palladium catalyst for the mild aerobic oxidation of 5-hydroxymethylfurfural into 2,5-furandicarboxylic acid in water, *Catal. Sci. Technol.* 5 (2015) 3194–3202, <https://doi.org/10.1039/C4CY01407C>.
- [76] B. Liu, Y. Ren, Z. Zhang, Aerobic oxidation of 5-hydroxymethylfurfural into 2,5-furandicarboxylic acid in water under mild conditions, *Green Chem.* 17 (2015) 1610–1617, <https://doi.org/10.1039/C4GC02019G>.
- [77] Z. Zhang, J. Zhen, B. Liu, K. Lv, K. Deng, Selective aerobic oxidation of the biomass-derived precursor 5-hydroxymethylfurfural to 2,5-furandicarboxylic acid under mild conditions over a magnetic palladium nanocatalyst, *Green Chem.* 17 (2015) 1308–1317, <https://doi.org/10.1039/C4GC01833H>.
- [78] Y. Wang, K. Yu, D. Lei, W. Si, Y. Feng, L.-L. Lou, S. Liu, Basicity-tuned hydrotalcite-supported Pd catalysts for aerobic oxidation of 5-hydroxymethyl-2-

- furfural under mild conditions, *ACS Sustainable Chem. Eng.* 4 (2016) 4752–4761, <https://doi.org/10.1021/acssuschemeng.6b00965>.
- [79] H. Choudhary, K. Ebitani, Hydrotalcite-supported PdPt-catalyzed aerobic oxidation of 5-hydroxymethylfurfural to 2,5-furandicarboxylic acid in water, *Chem. Lett.* 45 (2016) 613–615, <https://doi.org/10.1246/cl.160178>.
- [80] K. Gupta, R.K. Rai, A.D. Dwivedi, S.K. Singh, Catalytic aerial oxidation of biomass-derived furans to furan carboxylic acids in water over bimetallic nickel-palladium alloy nanoparticles, *ChemCatChem* 9 (2017) 2760–2767, <https://doi.org/10.1002/cctc.201600942>.
- [81] Z. Zhang, K. Deng, Recent Advances in the catalytic synthesis of 2,5-furandicarboxylic acid and its derivatives, *ACS Catal.* 5 (2015) 6529–6544, <https://doi.org/10.1021/acscatal.5b01491>.
- [82] P. Vinke, H.E. van Dam, H. van Bekkum, Platinum catalyzed oxidation of 5-hydroxymethylfurfural, in: *Studies in Surface Science and Catalysis*, Elsevier, 1990: pp. 147–158, [https://doi.org/10.1016/S0167-2991\(08\)60144-5](https://doi.org/10.1016/S0167-2991(08)60144-5).
- [83] X. Li, Q. Xia, V.C. Nguyen, K. Peng, X. Liu, N. Essayem, Y. Wang, High yield production of HMF from carbohydrates over silica–alumina composite catalysts, *Catal. Sci. Technol.* 6 (2016) 7586–7596, <https://doi.org/10.1039/C6CY01628F>.
- [84] P. Verdeguer, N. Merat, A. Gaset, Oxydation catalytique du HMF en acide 2,5-furane dicarboxylique, *J. Mol. Catal.* 85 (1993) 327–344, [https://doi.org/10.1016/0304-5102\(93\)80059-4](https://doi.org/10.1016/0304-5102(93)80059-4).
- [85] H. Ait Rass, N. Essayem, M. Besson, Selective aqueous phase oxidation of 5-hydroxymethylfurfural to 2,5-furandicarboxylic acid over Pt/C catalysts: influence of the base and effect of bismuth promotion, *Green Chem.* 15 (2013) 2240–2251, <https://doi.org/10.1039/c3gc40727f>.

- [86] H. Ait Rass, N. Essayem, M. Besson, Selective aerobic oxidation of 5-HMF into 2,5-furandicarboxylic acid with Pt catalysts supported on TiO<sub>2</sub> - and ZrO<sub>2</sub> -based supports, *ChemSusChem* 8 (2015) 1206–1217, <https://doi.org/10.1002/cssc.201403390>.
- [87] Z. Miao, T. Wu, J. Li, T. Yi, Y. Zhang, X. Yang, Aerobic oxidation of 5-hydroxymethylfurfural (HMF) effectively catalyzed by a Ce<sub>0.8</sub> Bi<sub>0.2</sub> O<sub>2-δ</sub> supported Pt catalyst at room temperature, *RSC Adv.* 5 (2015) 19823–19829, <https://doi.org/10.1039/C4RA16968A>.
- [88] R. Sahu, P.L. Dhepe, Synthesis of 2,5-furandicarboxylic acid by the aerobic oxidation of 5-hydroxymethyl furfural over supported metal catalysts, *Reac. Kinet. Mech. Cat.* 112 (2014) 173–187, <https://doi.org/10.1007/s11144-014-0689-z>.
- [89] C. Ke, M. Li, G. Fan, L. Yang, F. Li, Pt nanoparticles supported on nitrogen-doped-carbon-decorated CeO<sub>2</sub> for base-free aerobic oxidation of 5-hydroxymethylfurfural, *Chem. Asian J.* 13 (2018) 2714–2722, <https://doi.org/10.1002/asia.201800738>.
- [90] X. Han, C. Li, Y. Guo, X. Liu, Y. Zhang, Y. Wang, N-doped carbon supported Pt catalyst for base-free oxidation of 5-hydroxymethylfurfural to 2,5-furandicarboxylic acid, *Appl. Catal. A: General* 526 (2016) 1–8, <https://doi.org/10.1016/j.apcata.2016.07.011>.
- [91] W. Niu, D. Wang, G. Yang, J. Sun, M. Wu, Y. Yoneyama, N. Tsubaki, Pt nanoparticles loaded on reduced graphene oxide as an effective catalyst for the direct oxidation of 5-hydroxymethylfurfural (HMF) to produce 2, 5-furandicarboxylic acid (FDCA) under mild conditions, *Bull. Chem. Soc, Japan* 87 (2014) 1124–1129, <https://doi.org/10.1246/bcsj.20140096>.
- [92] P. Sharma, M. Solanki, R.K. Sharma, Metal-functionalized carbon nanotubes for biomass conversion: base-free highly efficient and recyclable catalysts for aerobic

- oxidation of 5-hydroxymethylfurfural, *New J. Chem.* 43 (2019) 10601–10609, <https://doi.org/10.1039/C9NJ01555H>.
- [93] C. Zhou, W. Deng, X. Wan, Q. Zhang, Y. Yang, Y. Wang, Functionalized carbon nanotubes for biomass conversion: The base-free aerobic oxidation of 5-hydroxymethylfurfural to 2,5-furandicarboxylic acid over platinum supported on a carbon nanotube catalyst, *ChemCatChem* 7 (2015) 2853–2863, <https://doi.org/10.1002/cctc.201500352>.
- [94] H. Chen, J. Shen, K. Chen, Y. Qin, X. Lu, P. Ouyang, J. Fu, Atomic layer deposition of Pt nanoparticles on low surface area zirconium oxide for the efficient base-free oxidation of 5-hydroxymethylfurfural to 2,5-furandicarboxylic acid, *Appl. Catal. A: General* 555 (2018) 98–107, <https://doi.org/10.1016/j.apcata.2018.01.023>.
- [95] H. Yu, K.-A. Kim, M.J. Kang, S.Y. Hwang, H.G. Cha, Carbon support with tunable porosity prepared by carbonizing chitosan for catalytic oxidation of 5-hydroxymethylfurfural, *ACS Sustainable Chem. Eng.* 7 (2019) 3742–3748, <https://doi.org/10.1021/acssuschemeng.8b03775>.
- [96] X. Han, L. Geng, Y. Guo, R. Jia, X. Liu, Y. Zhang, Y. Wang, Base-free aerobic oxidation of 5-hydroxymethylfurfural to 2,5-furandicarboxylic acid over a Pt/C–O–Mg catalyst, *Green Chem* 18 (2016) 1597–1604, <https://doi.org/10.1039/C5GC02114F>.
- [97] W. Gong, K. Zheng, P. Ji, Platinum deposited on cerium coordination polymer for catalytic oxidation of hydroxymethylfurfural producing 2,5-furandicarboxylic acid, *RSC Adv.* 7 (2017) 34776–34782, <https://doi.org/10.1039/C7RA05427K>.
- [98] Y. Zhang, Z. Xue, J. Wang, X. Zhao, Y. Deng, W. Zhao, T. Mu, Controlled deposition of Pt nanoparticles on Fe<sub>3</sub>O<sub>4</sub> @carbon microspheres for efficient oxidation of 5-hydroxymethylfurfural, *RSC Adv.* 6 (2016) 51229–51237,

<https://doi.org/10.1039/C6RA06792A>.

- [99] S.E. Davis, A.D. Benavidez, R.W. Gosselink, J.H. Bitter, K.P. de Jong, A.K. Datye, R.J. Davis, Kinetics and mechanism of 5-hydroxymethylfurfural oxidation and their implications for catalyst development, *J. Mol. Catal. A: Chemical* 388–389 (2014) 123–132, <https://doi.org/10.1016/j.molcata.2013.09.013>.
- [100] J. Shen, H. Chen, K. Chen, Y. Qin, X. Lu, P. Ouyang, J. Fu, Atomic layer deposition of a Pt-skin catalyst for base-free aerobic oxidation of 5-hydroxymethylfurfural to 2,5-furandicarboxylic acid, *Ind. Eng. Chem. Res.* 57 (2018) 2811–2818, <https://doi.org/10.1021/acs.iecr.7b05101>.
- [101] <http://heraeus-edelmetallhandel.de>, accessed 07.08.2015 (see also Supporting Information), (n.d.).
- [102] G. Yi, S.P. Teong, Y. Zhang, Base-free conversion of 5-hydroxymethylfurfural to 2,5-furandicarboxylic acid over a Ru/C catalyst, *Green Chem.* 18 (2016) 979–983, <https://doi.org/10.1039/C5GC01584G>.
- [103] C.-T. Chen, C.V. Nguyen, Z.-Y. Wang, Y. Bando, Y. Yamauchi, M.T.S. Bazziz, A. Fatehmulla, W.A. Farooq, T. Yoshikawa, T. Masuda, Hydrogen peroxide assisted selective oxidation of 5-hydroxymethylfurfural in water under mild conditions, *ChemCatChem* 10 (2018) 361–365, <https://doi.org/10.1002/cctc.201701302>
- [104] F. Kerdi, H. Ait Rass, C. Pinel, M. Besson, G. Peru, B. Leger, S. Rio, E. Monflier, A. Ponchel, Evaluation of surface properties and pore structure of carbon on the activity of supported Ru catalysts in the aqueous-phase aerobic oxidation of HMF to FDCA, *Appl. Catal. A: General* 506 (2015) 206–219, <https://doi.org/10.1016/j.apcata.2015.09.002>.
- [105] J. Nie, J. Xie, H. Liu, Activated carbon-supported ruthenium as an efficient catalyst for selective aerobic oxidation of 5-hydroxymethylfurfural to 2,5-diformylfuran,

- Chin. J. Catal. 34 (2013) 871–875, [https://doi.org/10.1016/S1872-2067\(12\)60551-8](https://doi.org/10.1016/S1872-2067(12)60551-8).
- [106] J. Xie, J. Nie, H. Liu, Aqueous-phase selective aerobic oxidation of 5-hydroxymethylfurfural on Ru/C in the presence of base, Chin. J. Catal. 35 (2014) 937–944, [https://doi.org/10.1016/S1872-2067\(14\)60136-4](https://doi.org/10.1016/S1872-2067(14)60136-4).
- [107] L. Zheng, J. Zhao, Z. Du, B. Zong, H. Liu, Efficient aerobic oxidation of 5-hydroxymethylfurfural to 2,5-furandicarboxylic acid on Ru/C catalysts, Sci. China Chem. 60 (2017) 950–957, <https://doi.org/10.1007/s11426-016-0489-3>.
- [108] J. Nie, H. Liu, Aerobic oxidation of 5-hydroxymethylfurfural to 2,5-diformylfuran on supported vanadium oxide catalysts: Structural effect and reaction mechanism, Pure Appl. Chem. 84 (2011) 765–777, <https://doi.org/10.1351/PAC-CON-11-07-02>.
- [109] K. Pupovac, R. Palkovits, Cu/MgAl<sub>2</sub>O<sub>4</sub> as bifunctional catalyst for aldol condensation of 5-hydroxymethylfurfural and selective transfer hydrogenation, ChemSusChem 6 (2013) 2103–2110, <https://doi.org/10.1002/cssc.201300414>.
- [110] H. Liu, X. Cao, T. Wang, J. Wei, X. Tang, X. Zeng, Y. Sun, T. Lei, S. Liu, L. Lin, Efficient synthesis of bio-monomer 2,5-furandicarboxylic acid from concentrated 5-hydroxymethylfurfural or fructose in DMSO/H<sub>2</sub>O mixed solvent, J. Ind. Eng. Chem. 77 (2019) 209–214, <https://doi.org/10.1016/j.jiec.2019.04.038>.
- [111] N. Lucas, N.R. Kanna, A.S. Nagpure, G. Kokate, S. Chilukuri, Novel catalysts for valorization of biomass to value-added chemicals and fuels, J. Chem. Sci. 126 (2014) 403–413, <https://doi.org/10.1007/s12039-014-0577-0>.
- [112] J. Artz, R. Palkovits, Base-free aqueous-phase oxidation of 5-hydroxymethylfurfural over ruthenium catalysts supported on covalent triazine frameworks, ChemSusChem 8 (2015) 3832–3838, <https://doi.org/10.1002/cssc.201501106>.
- [113] C.M. Pichler, M.G. Al-Shaal, D. Gu, H. Joshi, W. Ciptonugroho, F. Schüth, Ruthenium supported on high-surface-area zirconia as an efficient catalyst for the

- base-free oxidation of 5-hydroxymethylfurfural to 2,5-furandicarboxylic acid, *ChemSusChem* 11 (2018) 2083–2090, <https://doi.org/10.1002/cssc.201800448>.
- [114] T. Gao, Y. Yin, W. Fang, Q. Cao, Highly dispersed ruthenium nanoparticles on hydroxyapatite as selective and reusable catalyst for aerobic oxidation of 5-hydroxymethylfurfural to 2,5-furandicarboxylic acid under base-free conditions, *Mol. Catal.* 450 (2018) 55–64, <https://doi.org/10.1016/j.mcat.2018.03.006>.
- [115] D.K. Mishra, H.J. Lee, J. Kim, H.-S. Lee, J.K. Cho, Y.-W. Suh, Y. Yi, Y.J. Kim, MnCo<sub>2</sub>O<sub>4</sub> spinel supported ruthenium catalyst for air-oxidation of HMF to FDCA under aqueous phase and base-free conditions, *Green Chem.* 19 (2017) 1619–1623, <https://doi.org/10.1039/C7GC00027H>.
- [116] T. Gao, J. Chen, W. Fang, Q. Cao, W. Su, F. Dumeignil, Ru/Mn<sub>x</sub>Ce<sub>1-y</sub>O<sub>y</sub> catalysts with enhanced oxygen mobility and strong metal-support interaction: Exceptional performances in 5-hydroxymethylfurfural base-free aerobic oxidation, *J. Catalysis* 368 (2018) 53–68, <https://doi.org/10.1016/j.jcat.2018.09.034>.
- [117] Y.Y. Gorbanev, S. Kegnæs, A. Riisager, Selective aerobic oxidation of 5-hydroxymethylfurfural in water over solid ruthenium hydroxide catalysts with magnesium-based supports, *Catal Lett.* 141 (2011) 1752–1760, <https://doi.org/10.1007/s10562-011-0707-y>.
- [118] Y.Y. Gorbanev, S. Kegnæs, A. Riisager, Effect of support in heterogeneous ruthenium catalysts used for the selective aerobic oxidation of HMF in water, *Top. Catal.* 54 (2011) 1318–1324, <https://doi.org/10.1007/s11244-011-9754-2>.
- [119] T. Ståhlberg, E. Eyjólfsdóttir, Y.Y. Gorbanev, I. Sádaba, A. Riisager, Aerobic oxidation of 5-(hydroxymethyl)furfural in ionic liquids with solid ruthenium hydroxide catalysts, *Catal Lett.* 142 (2012) 1089–1097, <https://doi.org/10.1007/s10562-012-0858-5>.

- [120] X. Han, C. Li, X. Liu, Q. Xia, Y. Wang, Selective oxidation of 5-hydroxymethylfurfural to 2,5-furandicarboxylic acid over  $\text{MnO}_x\text{-CeO}_2$  composite catalysts, *Green Chem.* 19 (2017) 996–1004, <https://doi.org/10.1039/C6GC03304K>.
- [121] K. Yamaguchi, K. Mori, T. Mizugaki, K. Ebitani, K. Kaneda, Creation of a monomeric Ru species on the surface of hydroxyapatite as an efficient heterogeneous catalyst for aerobic alcohol oxidation, *J. Am. Chem. Soc.* 122 (2000) 7144–7145, <https://doi.org/10.1021/ja001325i>.
- [122] K. Yamaguchi, N. Mizuno, Scope, kinetics, and mechanistic aspects of aerobic oxidations catalyzed by ruthenium supported on alumina, *Chem. Eur. J.* 9 (2003) 4353–4361, <https://doi.org/10.1002/chem.200304916>.
- [123] D.V. Bavykin, A.A. Lapkin, S.T. Kolaczkowski, P.K. Plucinski, Selective oxidation of alcohols in a continuous multifunctional reactor: Ruthenium oxide catalysed oxidation of benzyl alcohol, *Appl. Catal. A: General* 288 (2005) 175–184, <https://doi.org/10.1016/j.apcata.2005.04.042>.
- [124] Z. Yang, W. Qi, R. Su, Z. He, Selective synthesis of 2,5-diformylfuran and 2,5-furandicarboxylic acid from 5-hydroxymethylfurfural and fructose catalyzed by magnetically separable catalysts, *Energy Fuels* 31 (2017) 533–541, <https://doi.org/10.1021/acs.energyfuels.6b02012>.
- [125] W. Schroeder, L. Katz, The use of silver oxide in the preparation of diaryldiazomethanes, *J. Org. Chem.* 19 (1954) 718–720, <https://doi.org/10.1021/jo01370a003>.
- [126] T. Reichstein, Notiz über 5-oxymethyl-furfurol, *Helv. Chim. Acta* 9 (1926) 1066–1068, <https://doi.org/10.1002/hlca.192600901141>.
- [127] K.G.A. Busch, J.W. Clark, L.B. Genung, E.F. Schroeder, W.L. Evans, The mechanism of carbohydrate oxidation. XVIII. The oxidation of certain sugars with

- silver oxide in the presence of potassium hydroxide, *J. Org. Chem.* 1 (1936) 1–16, <https://doi.org/10.1021/jo01230a001>.
- [128] M. Liu, H. Wang, H. Zeng, C.-J. Li, Silver(I) as a widely applicable, homogeneous catalyst for aerobic oxidation of aldehydes toward carboxylic acids in water—“silver mirror”: From stoichiometric to catalytic, *Sci. Adv.* 1 (2015) e1500020, <https://doi.org/10.1126/sciadv.1500020>.
- [129] J. An, G. Sun, H. Xia, Aerobic oxidation of 5-hydroxymethylfurfural to high-yield 5-hydroxymethyl-2-furancarboxylic acid by poly(vinylpyrrolidone)-capped Ag nanoparticle catalysts, *ACS Sustainable Chem. Eng.* 7 (2019) 6696–6706, <https://doi.org/10.1021/acssuschemeng.8b05916>.
- [130] G.D. Yadav, R.V. Sharma, Biomass derived chemicals: Environmentally benign process for oxidation of 5-hydroxymethylfurfural to 2,5-diformylfuran by using nano-fibrous Ag-OMS-2-catalyst, *Appl. Catal. B: Environmental* 147 (2014) 293–301, <https://doi.org/10.1016/j.apcatb.2013.09.004>.
- [131] D. Zhao, D. Rodríguez-Padrón, R. Luque, C. Len, Insights into the selective oxidation of 5-hydroxymethylfurfural to 5-hydroxymethyl-2-furancarboxylic acid using silver oxide, *ACS Sustainable Chem. Eng.* 8 (2020) 8486–8495, <https://doi.org/10.1021/acssuschemeng.9b07170>.
- [132] W. Tang, X. Wu, D. Li, Z. Wang, G. Liu, H. Liu, Y. Chen, Oxalate route for promoting activity of manganese oxide catalysts in total VOCs’ oxidation: effect of calcination temperature and preparation method, *J. Mater. Chem. A.* 2 (2014) 2544–2554, <https://doi.org/10.1039/C3TA13847J>.
- [133] E. Hayashi, T. Komanoya, K. Kamata, M. Hara, Heterogeneously-catalyzed aerobic oxidation of 5-hydroxymethylfurfural to 2,5-furandicarboxylic acid with MnO<sub>2</sub>, *ChemSusChem* 10 (2017) 654–658, <https://doi.org/10.1002/cssc.201601443>.

- [134] E. Hayashi, Y. Yamaguchi, K. Kamata, N. Tsunoda, Y. Kumagai, F. Oba, M. Hara, Effect of MnO<sub>2</sub> crystal structure on aerobic oxidation of 5-hydroxymethylfurfural to 2,5-furandicarboxylic Acid, *J. Am. Chem. Soc.* 141 (2019) 890–900, <https://doi.org/10.1021/jacs.8b09917>.
- [135] X. Han, C. Li, X. Liu, Q. Xia, Y. Wang, Selective oxidation of 5-hydroxymethylfurfural to 2,5-furandicarboxylic acid over MnO<sub>x</sub> – CeO<sub>2</sub> composite catalysts, *Green Chem.* 19 (2017) 996–1004, <https://doi.org/10.1039/C6GC03304K>.
- [136] F. Neațu, R.S. Marin, M. Florea, N. Petrea, O.D. Pavel, V.I. Pârvulescu, Selective oxidation of 5-hydroxymethyl furfural over non-precious metal heterogeneous catalysts, *Appl. Catal. B: Environmental* 180 (2016) 751–757, <https://doi.org/10.1016/j.apcatb.2015.07.043>.
- [137] A.B. Gawade, A.V. Nakhate, G.D. Yadav, Selective synthesis of 2,5-furandicarboxylic acid by oxidation of 5-hydroxymethylfurfural over MnFe<sub>2</sub>O<sub>4</sub> catalyst, *Catal. Today* 309 (2018) 119–125, <https://doi.org/10.1016/j.cattod.2017.08.061>.
- [138] B. Liu, Z. Zhang, K. Lv, K. Deng, H. Duan, Efficient aerobic oxidation of biomass-derived 5-hydroxymethylfurfural to 2,5-diformylfuran catalyzed by magnetic nanoparticle supported manganese oxide, *Appl. Catal. A: General* 472 (2014) 64–71, <https://doi.org/10.1016/j.apcata.2013.12.014>.
- [139] F. Neațu, N. Petrea, R. Petre, V. Somoghi, M. Florea, V.I. Parvulescu, Oxidation of 5-hydroxymethyl furfural to 2,5-diformylfuran in aqueous media over heterogeneous manganese based catalysts, *Catal. Today* 278 (2016) 66–73, <https://doi.org/10.1016/j.cattod.2016.03.031>.
- [140] B. Sarmah, R. Srivastava, Selective two-step synthesis of 2,5-diformylfuran from monosaccharide, disaccharide, and polysaccharide using H-Beta and octahedral

- MnO<sub>2</sub> molecular sieves, *Mol. Catal.* 462 (2019) 92–103, <https://doi.org/10.1016/j.mcat.2018.11.001>.
- [141] X. Zuo, A.S. Chaudhari, K. Snavely, F. Niu, H. Zhu, K.J. Martin, B. Subramaniam, Kinetics of homogeneous 5-hydroxymethylfurfural oxidation to 2,5-furandicarboxylic acid with Co/Mn/Br catalyst, *AIChE J.* 63 (2017) 162–171, <https://doi.org/10.1002/aic.15497>.
- [142] B. Saha, S. Dutta, M.M. Abu-Omar, Aerobic oxidation of 5-hydroxymethylfurfural with homogeneous and nanoparticulate catalysts, *Catal. Sci. Technol.* 2 (2012) 79–81, <https://doi.org/10.1039/C1CY00321F>.
- [143] A. Sanborn, Oxidation of furfural compounds, US008558018B2 (2013), n.d.
- [144] H. Zhou, H. Xu, Y. Liu, Aerobic oxidation of 5-hydroxymethylfurfural to 2,5-furandicarboxylic acid over Co/Mn-lignin coordination complexes-derived catalysts, *Appl. Catal. B: Environmental* 244 (2019) 965–973, <https://doi.org/10.1016/j.apcatb.2018.12.046>.
- [145] X. Zuo, P. Venkatasubramanian, D.H. Busch, B. Subramaniam, Optimization of Co/Mn/Br-catalyzed oxidation of 5-hydroxymethylfurfural to enhance 2,5-furandicarboxylic acid yield and minimize substrate burning, *ACS Sustainable Chem. Eng.* 4 (2016) 3659–3668, <https://doi.org/10.1021/acssuschemeng.6b00174>.
- [146] S. Zhang, X. Sun, Z. Zheng, L. Zhang, Nanoscale center-hollowed hexagon MnCo<sub>2</sub>O<sub>4</sub> spinel catalyzed aerobic oxidation of 5-hydroxymethylfurfural to 2,5-furandicarboxylic acid, *Catal. Commun.* 113 (2018) 19–22, <https://doi.org/10.1016/j.catcom.2018.05.004>.
- [147] K.T.V. Rao, J.L. Rogers, S. Souzanchi, L. Dessbesell, M.B. Ray, C.C. Xu, Inexpensive but highly efficient Co-Mn mixed-oxide catalysts for selective oxidation of 5-hydroxymethylfurfural to 2,5-furandicarboxylic acid, *ChemSusChem* 11 (2018)

3323–3334, <https://doi.org/10.1002/cssc.201800989>.

- [148] A. Jain, S.C. Jonnalagadda, K.V. Ramanujachary, A. Mugweru, Selective oxidation of 5-hydroxymethyl-2-furfural to furan-2,5-dicarboxylic acid over spinel mixed metal oxide catalyst, *Catal. Commun.* 58 (2015) 179–182, <https://doi.org/10.1016/j.catcom.2014.09.017>.
- [149] J. Deng, H.-J. Song, M.-S. Cui, Y.-P. Du, Y. Fu, Aerobic oxidation of hydroxymethylfurfural and furfural by using heterogeneous  $\text{Co}_x\text{O}_y$ -N@C Catalysts, *ChemSusChem* 7 (2014) 3334–3340, <https://doi.org/10.1002/cssc.201402843>.
- [150] H. Zhou, H. Xu, X. Wang, Y. Liu, Convergent production of 2,5-furandicarboxylic acid from biomass and  $\text{CO}_2$ , *Green Chem.* 21 (2019) 2923–2927, <https://doi.org/10.1039/C9GC00869A>.
- [151] L. Gao, K. Deng, J. Zheng, B. Liu, Z. Zhang, Efficient oxidation of biomass derived 5-hydroxymethylfurfural into 2,5-furandicarboxylic acid catalyzed by Merrifield resin supported cobalt porphyrin, *Chem. Eng. J.* 270 (2015) 444–449, <https://doi.org/10.1016/j.cej.2015.02.068>.
- [152] M.L. Ribeiro, U. Schuchardt, Cooperative effect of cobalt acetylacetonate and silica in the catalytic cyclization and oxidation of fructose to 2,5-furandicarboxylic acid, *Catal. Commun.* 4 (2003) 83–86, [https://doi.org/10.1016/S1566-7367\(02\)00261-3](https://doi.org/10.1016/S1566-7367(02)00261-3).
- [153] J. Ma, Z. Du, J. Xu, Q. Chu, Y. Pang, Efficient aerobic oxidation of 5-hydroxymethylfurfural to 2,5-diformylfuran, and synthesis of a fluorescent material, *ChemSusChem* 4 (2011) 51–54, <https://doi.org/10.1002/cssc.201000273>.
- [154] X. Tong, L. Yu, H. Chen, X. Zhuang, S. Liao, H. Cui, Highly efficient and selective oxidation of 5-hydroxymethylfurfural by molecular oxygen in the presence of Cu-MnO<sub>2</sub> catalyst, *Catal. Commun.* 90 (2017) 91–94, <https://doi.org/10.1016/j.catcom.2016.11.024>.

- [155] X. Tong, Y. Sun, X. Bai, Y. Li, Highly efficient aerobic oxidation of biomass-derived 5-hydroxymethyl furfural to produce 2,5-diformylfuran in the presence of copper salts, *RSC Adv.* 4 (2014) 44307–44311, <https://doi.org/10.1039/C4RA07181F>.
- [156] J. Ren, K. Song, Z. Li, Q. Wang, J. Li, Y. Wang, D. Li, C.K. Kim, Activation of formyl C H and hydroxyl O H bonds in HMF by the CuO(1 1 1) and Co<sub>3</sub>O<sub>4</sub>(1 1 0) surfaces: A DFT study, *Appl. Surface Sci.* 456 (2018) 174–183, <https://doi.org/10.1016/j.apsusc.2018.06.120>.
- [157] M. Ventura, M. Aresta, A. Dibenedetto, Selective Aerobic Oxidation of 5-(hydroxymethyl)furfural to 5-formyl-2-furancarboxylic acid in water, *ChemSusChem* 9 (2016) 1096–1100, <https://doi.org/10.1002/cssc.201600060>.
- [158] T.S. Hansen, I. Sádaba, E.J. García-Suárez, A. Riisager, Cu catalyzed oxidation of 5-hydroxymethylfurfural to 2,5-diformylfuran and 2,5-furandicarboxylic acid under benign reaction conditions, *Appl. Catal. A: General* 456 (2013) 44–50, <https://doi.org/10.1016/j.apcata.2013.01.042>.
- [159] X. Liu, J. Xiao, H. Ding, W. Zhong, Q. Xu, S. Su, D. Yin, Catalytic aerobic oxidation of 5-hydroxymethylfurfural over VO<sup>2+</sup> and Cu<sup>2+</sup> immobilized on amino functionalized SBA-15, *Chem. Eng. J.* 283 (2016) 1315–1321, <https://doi.org/10.1016/j.cej.2015.08.022>.
- [160] S. Mannam, G. Sekar, CuCl catalyzed selective oxidation of primary alcohols to carboxylic acids with tert-butyl hydroperoxide at room temperature, *Tetrahedron Lett.* 49 (2008) 2457–2460, <https://doi.org/10.1016/j.tetlet.2008.02.031>.
- [161] I. Sádaba, Y.Y. Gorbanev, S. Kegnaes, S.S.R. Putluru, R.W. Berg, A. Riisager, Catalytic performance of zeolite-supported vanadia in the aerobic oxidation of 5-hydroxymethylfurfural to 2,5-diformylfuran, *ChemCatChem* 5 (2013) 284–293,

<https://doi.org/10.1002/cctc.201200482>.

- [162] C. Fang, J.-J. Dai, H.-J. Xu, Q.-X. Guo, Y. Fu, Iron-catalyzed selective oxidation of 5-hydroxymethylfurfural in air: A facile synthesis of 2,5-diformylfuran at room temperature, *Chin. Chem. Lett.* 26 (2015) 1265–1268, <https://doi.org/10.1016/j.ccllet.2015.07.001>.
- [163] D.X. Martínez-Vargas, J. Rivera De La Rosa, L. Sandoval-Rangel, J.L. Guzmán-Mar, M.A. Garza-Navarro, C.J. Lucio-Ortiz, D.A. De Haro-Del Río, 5-Hydroxymethylfurfural catalytic oxidation under mild conditions by Co (II), Fe (III) and Cu (II) salen complexes supported on SBA-15: Synthesis, characterization and activity, *Appl. Catal. A: General* 547 (2017) 132–145, <https://doi.org/10.1016/j.apcata.2017.08.035>.
- [164] A. Tirsoaga, M. El Fergani, V.I. Parvulescu, S.M. Coman, Upgrade of 5-hydroxymethylfurfural to dicarboxylic acids onto multifunctional-based Fe<sub>3</sub>O<sub>4</sub>@SiO<sub>2</sub> magnetic catalysts, *ACS Sustainable Chem. Eng.* 6 (2018) 14292–14301, <https://doi.org/10.1021/acssuschemeng.8b02962>.
- [165] B. Saha, D. Gupta, M.M. Abu-Omar, A. Modak, A. Bhaumik, Porphyrin-based porous organic polymer-supported iron(III) catalyst for efficient aerobic oxidation of 5-hydroxymethyl-furfural into 2,5-furandicarboxylic acid, *J. Catal.* 299 (2013) 316–320, <https://doi.org/10.1016/j.jcat.2012.12.024>.
- [166] S. Wang, Z. Zhang, B. Liu, Catalytic Conversion of fructose and 5-hydroxymethylfurfural into 2,5-furandicarboxylic acid over a recyclable Fe<sub>3</sub>O<sub>4</sub> – CoO<sub>x</sub> magnetite nanocatalyst, *ACS Sustainable Chem. Eng.* 3 (2015) 406–412, <https://doi.org/10.1021/sc500702q>.
- [167] Z. Zhang, B. Liu, K. Lv, J. Sun, K. Deng, Aerobic oxidation of biomass derived 5-hydroxymethylfurfural into 5-hydroxymethyl-2-furancarboxylic acid catalyzed by a

- montmorillonite K-10 clay immobilized molybdenum acetylacetonate complex, *Green Chem.* 16 (2014) 2762-2770, <https://doi.org/10.1039/c4gc00062e>.
- [168] S. Wang, B. Liu, Z. Yuan, Z. Zhang, Aerobic oxidation of 5-hydroxymethylfurfural into furan compounds over Mo-hydroxyapatite-encapsulated magnetic  $\gamma$ -Fe<sub>2</sub>O<sub>3</sub>, *J. Taiwan Inst. Chem. Eng.* 58 (2016) 92–96, <https://doi.org/10.1016/j.jtice.2015.06.002>.
- [169] S. Li, K. Su, Z. Li, B. Cheng, Selective oxidation of 5-hydroxymethylfurfural with H<sub>2</sub>O<sub>2</sub> catalyzed by a molybdenum complex, *Green Chem.* 18 (2016) 2122–2128, <https://doi.org/10.1039/C5GC01991E>.
- [170] Y. Yan, K. Li, J. Zhao, W. Cai, Y. Yang, J.-M. Lee, Nanobelt-arrayed vanadium oxide hierarchical microspheres as catalysts for selective oxidation of 5-hydroxymethylfurfural toward 2,5-diformylfuran, *Appl. Catal. B: Environmental* 207 (2017) 358–365, <https://doi.org/10.1016/j.apcatb.2017.02.035>.
- [171] S.K. Hanson, R. Wu, L.A. “Pete” Silks, mild and selective vanadium-catalyzed oxidation of benzylic, allylic, and propargylic alcohols using air, *Org. Lett.* 13 (2011) 1908–1911, <https://doi.org/10.1021/ol103107v>.
- [172] J. Nie, H. Liu, Aerobic oxidation of 5-hydroxymethylfurfural to 2,5-diformylfuran on supported vanadium oxide catalysts: Structural effect and reaction mechanism, *Pure Appl. Chem.* 84 (2011) 765–777, <https://doi.org/10.1351/PAC-CON-11-07-02>.
- [173] F.L. Grasset, B. Katryniok, S. Paul, V. Nardello-Rataj, M. Pera-Titus, J.-M. Clacens, F. De Campo, F. Dumeignil, Selective oxidation of 5-hydroxymethylfurfural to 2,5-diformylfuran over intercalated vanadium phosphate oxides, *RSC Adv.* 3 (2013) 9942-9948, <https://doi.org/10.1039/c3ra41890a>.
- [174] R. Chen, J. Xin, D. Yan, H. Dong, X. Lu, S. Zhang, Highly efficient oxidation of 5-hydroxymethylfurfural to 2,5-furandicarboxylic acid with heteropoly acids and ionic

- liquids, *ChemSusChem* 12 (2019) 2715–2724, <https://doi.org/10.1002/cssc.201900651>.
- [175] S. Yan, Y. Li, P. Li, T. Jia, S. Wang, X. Wang, Fabrication of mesoporous POMs/SiO<sub>2</sub> nanofibers through electrospinning for oxidative conversion of biomass by H<sub>2</sub>O<sub>2</sub> and oxygen, *RSC Adv.* 8 (2018) 3499–3511, <https://doi.org/10.1039/C7RA12842H>.
- [176] Y. Li, Y. Li, P. Li, P. Cao, X. Wang, H. Guan, POM@surf(n)/CeO<sub>2</sub> electrospun nanofibers for the facile oxidation of 5-HMF to DFF, *Appl. Catal. A: General* 583 (2019) 117122, <https://doi.org/10.1016/j.apcata.2019.117122>.
- [177] C.V. Nguyen, Y.-T. Liao, T.-C. Kang, J.E. Chen, T. Yoshikawa, Y. Nakasaka, T. Masuda, K.C.-W. Wu, A metal-free, high nitrogen-doped nanoporous graphitic carbon catalyst for an effective aerobic HMF-to-FDCA conversion, *Green Chem.* 18 (2016) 5957–5961, <https://doi.org/10.1039/C6GC02118B>.
- [178] H. Watanabe, S. Asano, S. Fujita, H. Yoshida, M. Arai, Nitrogen-Doped, Metal-Free Activated Carbon Catalysts for Aerobic Oxidation of Alcohols, *ACS Catal.* 5 (2015) 2886–2894, <https://doi.org/10.1021/acscatal.5b00375>.
- [179] G. Lv, H. Wang, Y. Yang, X. Li, T. Deng, C. Chen, Y. Zhu, X. Hou, Aerobic selective oxidation of 5-hydroxymethyl-furfural over nitrogen-doped graphene materials with 2,2,6,6-tetramethylpiperidin-oxyl as co-catalyst, *Catal. Sci. Technol.* 6 (2016) 2377–2386, <https://doi.org/10.1039/C5CY01149C>.
- [180] J. Zhao, D. Wu, W.Y. Hernández, W.-J. Zhou, M. Capron, V.V. Ordonsky, Non-metallic aerobic oxidation of alcohols over anthraquinone based compounds, *Appl. Catal. A: General* 590 (2020) 117277, <https://doi.org/10.1016/j.apcata.2019.117277>.
- [181] S. Verma, M.N. Nadagouda, R.S. Varma, Porous nitrogen-enriched carbonaceous material from marine waste: chitosan-derived carbon nitride catalyst for aerial

- oxidation of 5-hydroxymethylfurfural (HMF) to 2,5-furandicarboxylic acid, *Sci Rep.* 7 (2017) 13596, <https://doi.org/10.1038/s41598-017-14016-5>.
- [182] R. Cang, L.-Q. Shen, G. Yang, Z.-D. Zhang, H. Huang, Z.-G. Zhang, Highly selective oxidation of 5-hydroxymethylfurfural to 5-hydroxymethyl-2-furancarboxylic acid by a robust whole-cell biocatalyst, *Catalysts* 9 (2019) 526, <https://doi.org/10.3390/catal9060526>.
- [183] M. Sayed, S.-H. Pyo, N. Rehnberg, R. Hatti-Kaul, Selective oxidation of 5-hydroxymethylfurfural to 5-hydroxymethyl-2-furancarboxylic acid using *Gluconobacter oxydans*, *ACS Sustainable Chem. Eng.* 7 (2019) 4406–4413, <https://doi.org/10.1021/acssuschemeng.8b06327>.
- [184] F. Koopman, N. Wierckx, J.H. de Winde, H.J. Ruijsenaars, Efficient whole-cell biotransformation of 5-(hydroxymethyl)furfural into FDCA, 2,5-furandicarboxylic acid, *Bioresour. Technol.* 101 (2010) 6291–6296, <https://doi.org/10.1016/j.biortech.2010.03.050>.
- [185] Y.-Z. Qin, Y.-M. Li, M.-H. Zong, H. Wu, N. Li, Enzyme-catalyzed selective oxidation of 5-hydroxymethylfurfural (HMF) and separation of HMF and 2,5-diformylfuran using deep eutectic solvents, *Green Chem.* 17 (2015) 3718–3722, <https://doi.org/10.1039/C5GC00788G>.
- [186] M. Krystof, M. Pérez-Sánchez, P. Domínguez de María, Lipase-Mediated Selective Oxidation of Furfural and 5-Hydroxymethylfurfural, *ChemSusChem* 6 (2013) 826–830, <https://doi.org/10.1002/cssc.201200954>.
- [187] J. Carro, P. Ferreira, L. Rodríguez, A. Prieto, A. Serrano, B. Balcells, A. Ardá, J. Jiménez-Barbero, A. Gutiérrez, R. Ullrich, M. Hofrichter, A.T. Martínez, 5-hydroxymethylfurfural conversion by fungal aryl-alcohol oxidase and unspecific peroxygenase, *FEBS J.* 282 (2015) 3218–3229, <https://doi.org/10.1111/febs.13177>.

- [188] A. Serrano, E. Calviño, J. Carro, M.I. Sánchez-Ruiz, F.J. Cañada, A.T. Martínez, Complete oxidation of hydroxymethylfurfural to furandicarboxylic acid by aryl-alcohol oxidase, *Biotechnol. Biofuels* 12 (2019) 217, <https://doi.org/10.1186/s13068-019-1555-z>.
- [189] S.M. McKenna, P. Mines, P. Law, K. Kovacs-Schreiner, W.R. Birmingham, N.J. Turner, S. Leimkühler, A.J. Carnell, The continuous oxidation of HMF to FDCA and the immobilisation and stabilisation of periplasmic aldehyde oxidase (PaoABC), *Green Chem.* 19 (2017) 4660–4665, <https://doi.org/10.1039/C7GC01696D>.
- [190] W.P. Dijkman, M.W. Fraaije, Discovery and characterization of a 5-hydroxymethylfurfural oxidase from *Methylovorus* sp. strain MP688, *Appl. Environ. Microbiol.* 80 (2014) 1082–1090, <https://doi.org/10.1128/AEM.03740-13>.
- [191] W.P. Dijkman, D.E. Groothuis, M.W. Fraaije, Enzyme-catalyzed oxidation of 5-hydroxymethylfurfural to furan-2,5-dicarboxylic acid, *Angew. Chem.* 126 (2014) 6633–6636, <https://doi.org/10.1002/ange.201402904>.